EVALUATION OF AND STANDARDIZATION TESTS FOR A.C. SIGNAL MODIFIERS

by

Eugene C. Moss, Lieutenant, USN
B.S., U.S. Naval Academy, 1948
B.S., U.S. Navy Postgraduate School, 1954

William A. Teasley Jr., Lieutenant, USN
B.S., U.S. Naval Academy, 1946
B.S., U.S. Navy Postgraduate School, 1954

SUMITTED IN PARTIAL FULFILLMENT OF THE
REQUIREMENTS FOR THE DEGREE OF
MASTER OF SCIENCE

at the

MASSACHUSETTS INSTITUTE OF TECHNOLOGY

1955

Signature of Authors

Dept. of Aeronautical Engineering, May 23, 1955

Certified by

Thesis Supervisor

Chairman, Departmental Committee on Graduate Students

Thesis
1955

This thesis, written by the authors while affiliated with the Instrumentation Laboratory, M. I. T., has been reproduced by the offset process using printer's ink in accordance with the following basic authorization received by Dr. C. S. Draper, Director of the Instrumentation Laboratory.

COPY

April 7, 1950

Dr. C. S. Draper
33-103

Dear Dr. Draper:

Mr. L. E. Payne has shown to me a recent printed reproduction of a thesis, in this instance a Master's dissertation, submitted in partial fulfillment of the requirements for the degree of Master of Science at the Massachusetts Institute of Technology.

The sample shown is printed by the offset press using screened illustrations, graphs and other material. For the purposes of the Library which include record and permanent preservation, theses reproduced in this manner are perfectly satisfactory and in my opinion meet all of the physical requirements of the graduate school insofar as they pertain to the preparation of a thesis.

I note that in the sample submitted the signatures have been reproduced along with the text by photo lithography. It is suggested that for the Library record copy the author, thesis supervisor and chairman of the Departmental Committee on Graduate Students affix their signatures in writing as complete authorization of the study. These can be written above the reproduced signature if desired.

Sincerely yours,

(signed)

Vernon D. Tate
Director of Libraries

VDT/jl

cc: Dean Bunker
Mr. Payne

COPY

EVALUATION OF AND STANDARDIZATION TESTS FOR A.C. SIGNAL MODIFIERS

by

Eugene C. Moss

William A. Teasley Jr.

Submitted to the Department of Aeronautical Engineering on May 23, 1955, in partial fulfillment of the requirements for the degree of Master of Science.

ABSTRACT

Signal modifiers are a class of devices used as elements in electrical circuitry to alter the wave form of input signals. These input signals may exist as a varying voltage or as the modulation superimposed on an a.c. carrier voltage with a fixed frequency. The alteration may be interpreted from the standpoint of the harmonic content of the signal, i.e. in terms of the frequency analysis. From this standpoint signal modifiers alter phase and magnitude of the frequency components.

Three typical signal modifiers were tested and evaluated. To provide a better comparison, modifiers having somewhat the same type of frequency response were selected. In general the modifiers have a varying amount of phase lead over an appreciable frequency range. The modifiers are of the type

(a) demodulator - RC modifier - remodulator,

(b) parallel "T" RC modifier, and

(c) chopper - RC modifier.

In general it was found that (a) provides better over all frequency response characteristics. (b) provides a smaller package with small reduction in frequency response for change in carrier frequency. (c) provides better low frequency response.

A standard method of measuring signal phase and magnitude is suggested in the introduction.

Thesis Supervisor: Sidney Lees
Title: Assistant Professor of Aeronautical Engineering

May 23, 1955

Professor Leicester F. Hamilton
Secretary of the Faculty
Massachusetts Institute of Technology
Cambridge 39, Massachusetts

Dear Professor Hamilton:

In accordance with the regulations of the faculty, we hereby submit a thesis entitled Evaluation of and Standardization Tests for A.C. Signal Modifiers in partial fulfillment of the requirements for the degree of Master of Science without specification.

Eugene C. Moss

William A. Teasley Jr.

ACKNOWLEDGEMENT

The authors express their appreciation to the personnel of the Instrumentation Laboratory, Massachusetts Institute of Technology who assisted in the preparation of this thesis. Particular thanks are due to Dr. Sidney Lees for his advice and guidance as thesis supervisor.

The authors express a special appreciation to their wives who, for three years, with patience and understanding, have been looking forward to the day they could read the printed version of this thesis.

The graduate work for which this thesis is a partial requirement was performed while the authors were assigned to the Naval Administrative Unit, Massachusetts Institute of Technology.

TABLE OF CONTENTS

LIST OF ILLUSTRATIONS

OBJECT

The object of this thesis is to evaluate several alternating current signal modifiers and to develop a standardized measuring technique upon which this evaluation is to be based.

CHAPTER 1

INTRODUCTION

As mentioned briefly in the abstract, uses for signal modifiers are found in electric and electronic circuitry. The shaping of signal frequency responses is of paramount importance in servomechanisms and systems using feedback control. Computing circuits using analogue or digital computing elements frequently require signal mofifying devices. Communication and radio circuitry have many and varied uses of wave shaping networks such as signal modifiers. In many ideal systems it is generally desired that the output signal be an exact replica of the input (power amplified as desired) with no time delays. For sinusoidal inputs, the output would have flat magnitude characteristics and zero phase shift throughout the designed frequency range. In actual systems involving electro-mechanical, hydraulic, pneumatic, etc., elements, there are natural and unavoidable time delays accompanied by magnitude attenuation. Time delay and attenuation give rise to system instability with oscillating signal outputs. In an effort to minimize these delays, signal modifiers with phase lead characteristics are introduced. It is the general need of these systems for lead type networks that suggested this study of ways and means for evaluating basic types of signal modifiers. In the evaluation a technique for a standard method of measuring phase angle and magnitude change is suggested.

In many systems the input signal to the lead modifier is in the form of a modulated suppressed-carrier voltage. It is usually required that the modifier output signal be of the same form with the same carrier frequency as the input. With this in mind, the signal may be operated on by either of two general types of modifiers. It may

first be demodulated, operated on, and remodulated. In the demodulated state the signal is modified using d.c. modifiers [1, 4, 5]. Or, it may be operated on directly in the a.c. state. Modifiers providing the first type of modification will be refered to as type I modifiers and the others as type II modifiers [7].

Three basic modifiers of the above types were selected for evaluation. The frequency function of each modifiers is as follows:

(a) type I, demodulation - remodulation (chapter 2)

$$\frac{1}{1 + (CT)_{(lg)(1)}\, j\, w_d} \times \frac{1 + (CT)_{(ld)}\, j\, w_d}{1 + \frac{(CT)_{(lg)(2)}}{K}\, j\, w_d}$$

(b) type II, parallel "T" RC network (chapter 3)

$$\frac{1 + (CT)_{(ld)}\, j\, w_d}{1 + (CT)_{(lg)}\, j\, w_d}$$

(c) type II, chopper RC network (chapter 4)

$$\frac{(CT)_{(ld)}\, j\, w_d}{1 + (CT)_{(lg)}\, j\, w_d}$$

w_d represents the frequency of modulation. $(CT)_{(ld)}$ and $(CT)_{(lg)}$ are time constants selected considering the response characteristics desired. K is a constant determining the magnitude gain and maximum phase lead for the network. In evaluation of these modifiers general and specific comparisons are advanced. The qualtities desired in a particular modifier will dictate the superiority of one over the other.

Generally the noise problem appears to be about the same for all modifiers. The amount of electrical noise tolerable depends primarily on the sensitivity of the control or actuating elements in the system. Thus, only the noise to signal ratio is estimated without attempt to determine its detrimental effect. Noise may emanate from several sources, such as backlash in gears, voltage variations, harmonic components of carrier frequency originating at the carrier source or at the synchros in the signal generator, atmospheric pickup, or

spurious signals due to stray inductive and capacitive effects. It is manifested somewhat differently in each modifier. The primary noise in the type I modifier is brought about by rectification in the demodulator. This is commonly called ripple and is indirectly related to the amount of smoothing done by filter networks accompanying the demodulator. In the parallel "T" network of type II modifier noise shows up in the form of a second envelope in quadrature to the signal envelope. It is proportional to the amount of shift of carrier frequency from the tuned frequency of the modifier. Carrier harmonics are more evident in type II modifiers and require special filtering in some cases. In all modifiers the output signal is badly distorted with noise at the low end of the signal frequency range. The minimum magnitude gain occurs at the low frequencies. This puts the signal in the region of spurious pickup noise. To reduce noise special filtering is required as mentioned. Filter circuits added to the demodulation-remodulation modifier reduce noise magnitude. Unfortunately the reduction is accompanyed by a time delay or an effective phase lag of the modulating signal envelope. This lag may be compensated by increasing the attenuation constant K which, however, results in increase of overall noise-to-signal ratio. Thus a compromise must be reached in the amount of phase lead obtainable and the amount of noise tolerable. High harmonic frequency noise in type II parallel "T" modifier can be removed by special filtering. As before, the addition of filters causes a reduction in signal magnitude. At low frequencies this reduction puts the signal magnitude level in the region of spurious pickup noise. Thus, a compromise must be made between magnitude attenuation and amount of noise tolerable. Noise in the type II chopper RC modifier cannot be compared on the same basis. The output of this modifier is one half of the envelope of a modulated suppressed carrier wave. The waves of carrier frequency are not sinusoids but a segment of an exponential decay. This type signal somewhat limits a general discussion of its noise. At the same time, this type of signal is somewhat limited in application.

The one singular advantage of type II modification is that it may be obtained with considerably less equipment than type I. A packaged modifier is obtainable involving less weight, space, and maintenance

requirements [6]. With this advantage, however, the type II modifier suffers magnitude and phase lead reduction for change of carrier frequency. This pertains only to the parallel "T", as the effect of carrier frequency shift was not investigated for the chopper RC modifier.

Due to phase lead fall off at low frequencies, the demodulation-remodulation and parallel "T" modifiers, are not particularly adaptable for systems requiring good low frequency response. In this respect the chopper RC modifier does provide a large amount of useful phase lead at low modulation frequencies. There is an upper frequency limit for useful phase lead for all modifiers. This upper limit is dictated by the denominator time constants in the frequency functions. The numerator and denominator time constants may be shifted arbitrarily to extend the region of useful phase lead with consequential change in magnitude. That is, magnitude attenuation is increased with the extension of the phase lead region.

Appendix B contains the frequency response curves for all the modifiers evaluated. The regions of phase lead appear somewhat limited frequency-wise. The network RC parameters were intentionally adusted to provide an observable variance of response over the available range of modulation frequency. This range was limited by the range of the Graham Variable Speed Drive used. A modulated suppressed carrier signal was the input and output signal for all curves.

The smoothing filters in the type I modifier introduces phase lag which must be considered in the overall compensation. That is, the overall phase lead and magnitude gain is reduced somewhat. The response of this modifier is not sensitive to a change of carrier frequency.

The response curves for the type II parallel "T" modifier show a reduction in phase lead for a change in carrier frequency from the tuned frequency of the modifier. With the exception of this reduction, the modifier cannot tell the difference between a change in carrier frequency or a change in modulation frequency. That is, the frequency function of the modifier is not substantially changed for a shift in carrier frequency. The sum of modulation frequency and change in carrier frequency up to 4 cps can be tolerated without failure of the

modifier to produce useful phase lead. Above 4 cps the modifier introduces phase lag. This limit of 4 cps will be different for changes in the RC network parameters. The response curves show how well the modifier approximates the first order form of the frequency function. This approximation is good up to a sum of modulation frequency and change in carrier frequency of about 10 to 12 cps. Beyond this, the second order form of the frequency function must be used.

$$\frac{\frac{(j w)^2}{w_o^2} + \frac{2 j w}{w_o^2 (CT)_{(ld)}} + 1}{\frac{(j w)^2}{w_o^2} + \frac{2 j w}{w_o^2 (CT)_{(lg)}} + 1}$$

w_o is the tuned frequency of the modifier. This limit, too, is a function of the RC parameters of the network. Addition of noise filters to the parallel "T" modifier tended to load down the input and output to the extent that the tuned frequency shifted from the designed value of 60 cps to about 59 1/2 cps.

The response curves of the type II chopper RC modifier show the large amount of phase lead at low modulation frequency. But there is a departure in the phase response from the $\frac{(CT)_{(ld)} j w_d}{1+(CT)_{(lg)} j w_d}$ frequency function. This is accounted for by the dwell time during the charging period; the time it takes the reed to break the charging contact and make the discharging contact, and one half of the dwell time of the discharging period. This last interval must be considered because the chopper RC network concerns itself with average values. The total time interval becomes a larger percentage of the period as w_d becomes larger. This means that as w_d gets larger, there is more phase lag introduced than is indicated in the general frequency function. However, amplitude is not affected by this increased lag.

Of several techniques [4] used during the experimental work to measure phase the one method found most successful is as follows: The stator leads of the control transformer in the signal generator are run to another control transformer. The latter control transformer

has its rotor calibrated to read angulor positions of the rotor. The rotor leads are then put into the horizontal deflection sweep of a cathode ray oscilloscope. If the output of the modulator is one half of a modulated suppressed carrier signal, as was the chopper RC signal modifier, it goes to the vertical deflection plates of the cathode ray oscilloscope. If the output of the remodulator is a fully modulated suppressed carrier wave, it is recommended that it be rectified by a rectifier whose frequency characteristics are known, to produce the same one half of a modulated suppressed carrier signal. Then the rectified wave is sent to the vertical deflection plates of the cathode ray oscilloscope as before. The resulting patterns can be easily interpreted if the signals are not badly distorted with noise. (see Figs. 4-5 and 4-6). Changing the rotor position of the measuring control transformer and observing the orientation of the pattern on the face of the oscilloscope, phase can be accurately read to within several degrees. Other methods of phase measurement [4] were attempted with much less success than the above.

Magnitude measurement was tried using a voltage calibrator in one instance and just reading squares on the face of the oscilloscope in the other. Counting the squares on the grid coordinate face of the oscilloscope is as accurate and easy as any other method [4].

C HAPTER 2

TYPE I A.C. SIGNAL MODIFICATION

2.1 It is often necessary to modify the correction signal in a servo loop. Where alternating current is used, this signal may be the output of a synchro generator-control transformer signal generator [1]. The output voltage of this device is

$$e_o(t) = E\cos w_d t \cos w_c t$$

where

$e_o(t)$ = output voltage of the control transformer.

w_d = modulation frequency in radians/sec. It is equal to the difference in the angular rates of rotation of the rotor of the synchro generator and the rotor of the control transformer.

w_c = carrier frequency in radians/sec. 377 radians/sec (60 cycles) is used.

One type of signal modification that may be desired is the development of phase lead. It is this problem that is investigated in this thesis.

One method of modifying the correction information is to rectify the output of the control transformer, filter the rectified signal, operate on the filtered signal, then remodulate the modified correction signal [4, 5]. It is this method of alternating current signal modification that McDonald [7] calls a type I system. It is the type I system that is discussed in this chapter. In contrast to the type I system, there is the more direct method of signal modification, such as the "notch" type R.C. network, that McDonald [7] calls a type II system. The type II systems are discussed in chapters 3 and 4.

2.2 Seely [9] shows that there is less noise, due to the presence of quadrature voltage, when the rectification is full wave compared to that of half wave. With full wave rectification Seely[9] also shows that there is a quadrature component present despite filtering. The magnitude of the quadrature voltage is related to the percentage of ripple present. However, the smoother the output of the filter, the more this output lags the input correction signal[11]. Therefore, a compromise must be reached between the quadrature disturbance permissible and the amount of lag tolerable for a particular correction signal frequency. The smoothing network and the lead modifier, chosen for this investigation, combine to give the performance function.

$$S_{(sm)[e;e]} \frac{CT_{(ld)}\ P + 1}{CT_{(lg_1)}P + 1\ \ CT_{(lg)_2}\ P + 1}$$

where

$S_{(sm)[e;e]}$ ≡ combined filter and lead modifier sensitivity

$CT_{(ld)}$ ≡ lead modifier lead characteristic time

$CT_{(lg)_1}$ ≡ smoothing filter lag characteristic time

$CT_{(lg)_2}$ ≡ lead modifier lag characteristic time

The frequency response for the whole system is plotted in Figs. B-2, 3.

2.3 As indicated in Figs. A-2, a Graham Variable Speed Drive is used to turn the rotor of the synchro generator. The drive has an indicating dial and a vernier scale. The dial and scale were calibrated in cycles per second and this calibration is shown in Fig. B-1. The stator leads of the synchro generator go to the stator posts of the control transformer. The rotor of the control transformer is clamped in place so that the rate of rotation of the Graham Variable Speed Drive provides the correction signal and therefore the modulation frequency, w_d, directly. The rotor leads of the control transformer provide the input signal to the rectifier. Circuit parameters were chosen to provide the compromise indicated in section 2.2. The

criterion was the ability to generate a demonstrable amount of phase lead within the range of the Graham Drive.

It was decided to use the chopper as a full wave rectifier [4] and a modified diode bridge as a modulator. The operation of the bridge is explained in Appendix D. There is a finite interval, during which the reed of the chopper is not touching either contact. It was felt that this interval was too long to use the chopper as a modulator. This led to the development of the modified diode bridge. It has been learned subsequent to this development that one form of this bridge has been used before, [12] but it is believed that the use of resistors in the input and output circuits are new. By using resistors, phase shift, due to modulation, is minimized. The diode bridge has the advantage over a triode modulator in that it is almost independent of tube characteristics. (See Appendix D)

Amplitude measurements were made with a Heathkit Voltage Calibrator and were made peak to peak. (See Fig. A-1) The output of the modulator goes to the input of the voltage calibrator. The output of the voltage calibrator goes to "Y" sweep of the oscilloscope. The voltage calibrator is switched between "signal" and "multiplier". The voltage scale of the calibrator is adjusted to match the amplitude of the signal's sweep and the voltage scale is read directly. The signal's sweep is maintained by the persistency of the cathode ray tube. Although the amplitudes plotted in Fig. B-2 indicate the validity of this method of measurement, it was found in the Type II system, that it was just as easy to count squares on the face of the oscilloscope.

Phase measurements were made as follows: [4]
the stator leads from the control transformer of the signal comparator are attached to the stator of a phase measuring control transformer. The rotor of this phase measuring control transformer has a pointer and a direct reading dial. The rotor leads go to the "X" sweep of the oscilloscope when phase is being measured. This technique permits the phase of the correction signal at the output to the modulator to be compared with the phase of the correction signal at the input of the rectifier. The input and output correction signals are nulled by positioning the rotor of the phase measuring control transformer. A pattern is produced similar to those of Figs. 4-5, 6, with the except-

ion that the horizontal line shown in these pictures are not present in this measurement. The amount of phase shift between input and output correction signal is read directly on the dial.

2.4 Figs. 2-1A, B, and C show the correction signal at different points in the circuit for the circuit parameters indicated in the figures. Fig. 2-1A shows that the output of the smoothing filter contains about 10% ripple for data frequency, w_d , = 12.03 radians/ sec. The lead modifier increases this percentage ripple to about 30% as shown in fig. 2-1B. While it may seem as though the percentage ripple in the remodulated signal is about the same in Fig. 2-1C, the square nature of the output carrier, as shown in Fig. 2-11, causes this appearance. Actually the percentage has been reduced to about 20% ripple when seen on the oscilloscope. The reduction of the percentage ripple, which is really the reduction of the quadrature component of the voltage, is the result of the switching action [4] of the diode bridge.

The values of the smoothing filter resistors were varied and the appearance of the output of the modulator was observed. It is noted that as the value of the resistance is increased, the general appearance of the modulated signal is much smoother. Figs. 2-2, 3 and 4 show this effect. Fig. 2-2 shows the output of the system for the circuit parameters whose response is plotted in Fig. B-2, 3. The ripple of the output is a little less than 10% . It is to be noted that there is a little reduction in ripple content in Fig. 2-4. However, for the lead modifier chosen, no phase lead was developed for the smoothing filter resistor = 150 K . For a smoothing filter resistor whose value is 1K, Fig. 2-3 shows that the ouput has about 30% ripple on one half of the modulated modified wave. On the other half of the modulated wave there is evidence of extreme distortion. The value of the condenser in the smoothing filter is increased to 14 MFD in Fig. 2-5. The ripple is reduced to about 5%. But with this value of capacitance it was not possible to develop lead.

The effect of unbalance of the input potentiometer in the rectifying circuit was investigated. Figs. 2-6 A, B, and C shows that the output of the smoothing filter has about 20% ripple; the output of the lead modifier shows about 60% ripple; and the output of the remodulator has about 25% ripple.

Figs. 2-7A and B shows that for a small phase shift in the chopper excitation voltage, 15 degrees, there is little increase in the signal ripple. Figs. 2-7A and B compare favorably with Figs. 2-1A and C.

The quality of the low modulating frequency signal is of interest. Fig. 2-8 indicates that there is almost 40% ripple and noise on the output signal for w_d = 2.5 radians/ sec. This compares to about 20% ripple for w_d = 12.0 radians/ sec. Fig. 2-9 shows that a smoothing filter resistor of 5K, at w_d = 2.5 radians/ sec, in addition to about 40% ripple and noise there is distortion introduced in the signal.

2.5 The conclusions drawn are as follows:

(a) In order to obtain at least 50^o lead over a range larger than 1.8 cycles with a signal containing less than 10% ripple, a frequency larger than 60 cycles is recommended.

(b) For any circuit parameters that produce lead for one cycle or more, with a signal containing less than 10% ripple at w_d = 12 radians/ sec, there is almost 40% noise and ripple superimposed on the signal for frequencies in the vicinity of w_d = 2 radians/ sec.

(c) A phase difference up to 15^o between the chopper excitation voltage and the signal carrier voltage does not seriously increase the noise on the signal.

(d) Unbalance of the input potentiometer can double the noise level of the signal.

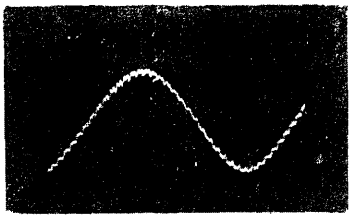

Fig. 2-1A Demodulator Output for w_d = 12.03 Rads./sec and Demodulator Filter Parameters at R=16.5K and C = 4 MFD.

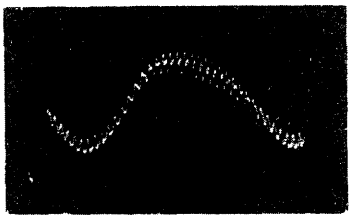

Fig. 2-1B Signal Modifier Output Signal.

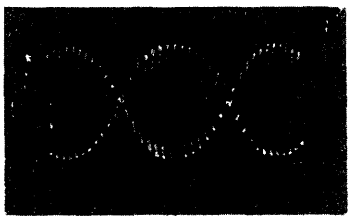

Fig. 2-1C Remodulator Output Signal.

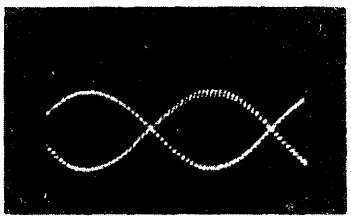

Fig. 2-2 Remodulator Output Signal for w_d = 6.35 Rads./sec and Demodulator Filter Parameters of R = 25K and C= 4 MFD.

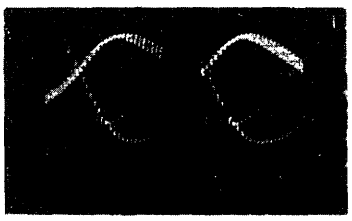

Fig. 2-3 Remodulator Output Signal for w_d = 6.35 Rads./sec and Demodulator Filter Parameters of R=1K and C=4 MFD.

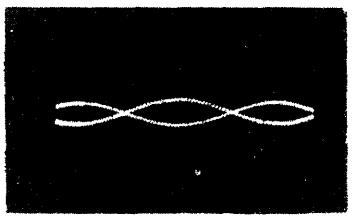

Fig. 2-4 Remodulator Output Signal for w_d = 6.35 Rads./sec and Demodulator Filter Parameters of R= 150K and C = 4 MFD.

The Type I System Output At Different Parts of the Circuit And for Various Circuit Parameters

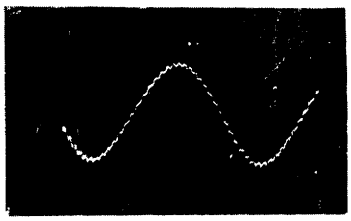

Fig. 2-5 Demodulator Output Signal for w_d = 12.03 Rads. / sec and Demodulator Filter Parameters of R= 25K and C= 14 MFD.

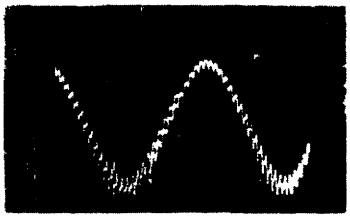

Fig. 2-6A Demodulator Output Signal for w_d = 12.03 Rads. /sec and Demodulator Filter Parameters of R = 10.0K and C = 4 MFD. Input Potentiometer to Demodulator is not Balanced.

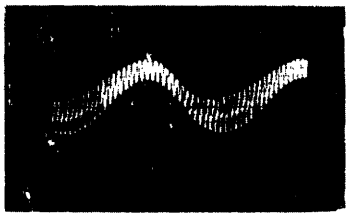

Fig. 2-6B Signal Modifier Output.

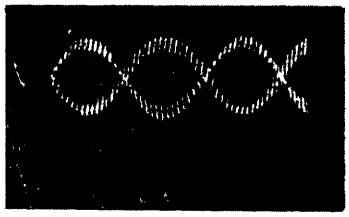

Fig. 2-6C Remodulator Output Signal.

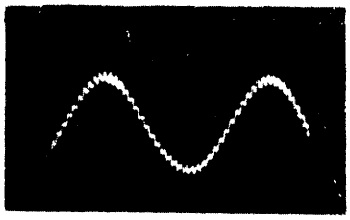

Fig. 2-7A Demodulator Output Signal for w_d = 12.03 Rads. /sec and Demodulator Filter Parameters of R = 16.5K and C = 4 MFD. Phase Shift Network to Demodulator Chopper Reference is Slightly Off Balance.

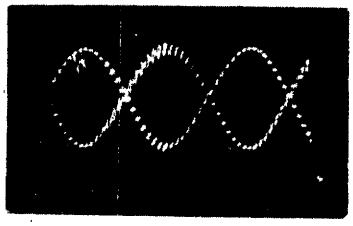

Fig. 2-7B Remodulator Output Signal.

The Type I System Output At Different Parts of the Circuit and for Various Circuit Parameters

Fig. 2-8 Remodulator Output Signal for w_d = 2.5 Rads./sec and Demodulator Filter Parameters of R = 16.5K and C = 4 MFD.

Fig. 2-9 Remodulator Output Signal for w_d = 2.5 Rads./sec and Demodulator Filter Parameters of R= 5K and C = 4 MFD.

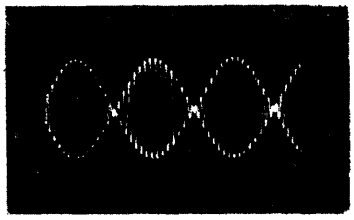

Fig. 2-10 Signal Generator Output for w_d = 12.03 Rads./sec.

Fig. 2-11 Remodulator Output Signal Carrier for w_d = 0 and Demodulator Filter Parameters of R = 25K and C = 4 MFD.

The Type I System Output at Different Parts of the Circuit and for Various Circuit Parameters

CHAPTER 3

THE PARALLEL "T" R C NETWORK AS A TYPE II A. C. SIGNAL MODIFIER

3.1 A method of signal modification of an a. c. carrier modulated signal employs a parallel "T" RC network (see Fig. A-6). Other networks providing the same type of modification are the bridge "T", series resonant RLC circuits, and the Wein Bridge. Because of their carrier frequency response characteristics (see Fig. B -4), these networks are sometimes referred to as "notch" networks [3, 5]. Considering the size, weight, and non-linearities of inductors series resonant RLC circuits are seldom used [4]. For practical networks the gains obtainable with the bridge "T" are considerably less than those of the parallel "T" [3]. The characteristics of the bridge "T", allow greater relative amplification of synchro third harmonic (to carrier frequency) [3]. Gains obtainable with the Wein Bridge are also less than those of the parallel"T" [3]. Considering the above, the parallel "T" network was chosen for the standard of type II signal modifiers. This chapter is devoted only to bringing out the salient features of the frequency response characteristics of the parallel "T", and postulating their effect in commonly used circuits. References (1), (2), and (3) were used as guides in the experimental work, in that they contain a thorough digest of information pertaining to the parallel "T" .

3.2 A signal modification often desired is the ideal proportional plus derivative characteristic.

$$[PF]_{(sm)}\,[e_{(in)}\,;\,e_{(out)}] \;=\; S_{(sm)}[e_{(in)};e_{(out)}]\,[FF]_{(sm)} \qquad (1)$$

where

$[PF]_{(sm)[e_{(in)}; e_{(out)}]}$ ≡ performance function of signal modifier for voltage input with voltage output.

$S_{(sm)[e_{(in)}; e_{(out)}]}$ ≡ sensitiveity of signal modifier primarily associated with the desired proportional term.

$[FF]_{(sm)}$ ≡ frequency function of the signal modifier associated primarily with the desired derivative term.

The frequency function providing the ideal modification has the form

$$[FF]_{(sm)} = 1 + (CT)_{(ld)}\, j\, (w-w_o) \qquad (2)$$

where

$(CT)_{(ld)}$ ≡ derivative time constant associated with the signal modifier parameters as will be shown later. $(CT)_{(ld)}$ is arbitrarily selected depending on the desired characteristics of the frequency response.

w_o ≡ the frequency of the input signal voltage.

w_o ≡ the tuned frequency of the signal modifier.

Let $(w-w_o)$ ≡ frequency of modulation.

Now if the input signal voltage is of the form

$$e_{(in)} = e(t) \cos (w_o\, t) \qquad (3)$$

of a suppressed carrier modulated signal,
where

$e(t)$ ≡ modulation voltage

t ≡ time,

then the signal modifier output voltage has the form

$$e_{(out)} = S_{(sm)} \left[e(t) + (CT)_{(ld)} \frac{de(t)}{dt} \cos w_o t \right] \qquad (4)$$

A parallel "T" network used for obtaining an approximation of the ideal proportional plus derivative characteristic may have the actual performance function [1, 3] of

$$[PF]_{(sm)[e_{(in)};\, e_{(out)}]} = \frac{(CT)_{(lg)}}{(CT)_{(ld)}} \left[\frac{1 + (CT)_{(ld)}\, j\left(\frac{w+w_o}{2w}\right)(w-w_o)}{1 + (CT)_{(lg)}\, j\left(\frac{w+w_o}{2w}\right)(w-w_o)} \right] \tag{5a}$$

where

$(CT)_{(lg)}$ = integral time constant arbitrarily selected considering the desired characteristics of the frequency response. Generally $(CT)_{(lg)} << (CT)_{(ld)}$ to minimize the time lag effect of the denominator and is usually less than $\frac{1}{w_o}$ [3].

The other symbols of equation (5a) are as defined before. If the modulating voltage of the input signal, e(t), does not have high frequency components of large amplitude then

$$\frac{w + w_o}{2w} \approx 1$$

Let the frequency of the modulating voltage be defined as before

$$w_d \equiv w - w_o$$

thus the performance function of the parallel "T" as a signal modifier simplifies to

$$[PF]_{(sm)[e_{(in)};e_{(out)}]} = \frac{(CT)_{(lg)}}{(CT)_{(ld)}} \left[\frac{1 + (CT)_{(ld)}\, j\, w_d}{1 + (CT)_{(lg)}\, j\, w_d} \right] \tag{6}$$

where

$$S_{(sm)[e_{(in)};\, e_{(out)}]} \equiv \frac{(CT)_{(lg)}}{(CT)_{(ld)}}, \text{ and}$$

$$[FF]_{(sm)} \equiv \frac{1 + (CT)_{(ld)}\, j\, w_d}{1 + (CT)_{(lg)}\, j\, w_d}.$$

It is noted that the frequency function of equation (6) is associated with the frequency of modulation of the signal voltage. It is also noted that

the forms assumed by equations (5a) and (6) are valid only within certain RC parameter restrictions as brought out in references (1) and (3).

Another form [1, 3] of the performance function of the parallel "T" is

$$[PF]_{(sm)[e_{(in)};\, e_{(out)}]} = \frac{[(CT)\,p + 1][\frac{1}{w_n^2}\,p^2 + \frac{2\zeta_n}{w_n}\,p + 1]}{[(CT)\,p + 1][\frac{1}{w_n^2}\,p^2 + \frac{2\zeta_n}{w_n}\,p + 1]} \qquad (5b)$$

where

$(CT) \equiv$ a time indeterminate such that the first order expressions in the numerator and denominator are equal, and thus may be cancelled.

$w_n \equiv$ the undamped natural frequency of the second order expressions in the numerator and denominator and is equal to w_o the tuned frequency of the parallel "T".

$\zeta_n \equiv$ the damping ratio of the numerator second order factor and is equal to the reciprocal product of the derivative time constant and the tuned frequency of the parallel "T", $\frac{1}{(CT)_{(ld)}\, w_n}$.

$\zeta_d \equiv$ the damping ratio of the denominator second order factor and is equal to the reciprocal product of the integral time constant and tuned frequency of the parallel "T", $\frac{1}{(CT)_{(lg)}\, w_n}$.

$p \equiv$ the operator $\frac{d}{dt}$.

If p is replaced by (jw) and appropriate substitutions made, equation (5b) may be algebraically manipulated to appear in the form of equation (5a). The two forms are equivalent. The advantages in use of either form for design and frequency response analysis will be discussed in the conclusions at the end of this chapter. The characteristic time constants, (CT), in equation (5b) are equal. The first order factors cancel. This reduces the performance function to the ratio of two second order factors. The cancellation does not effect the characteristics of the frequency function, but does effect the input and output

impedances of the network [3]. The restrictions imposed on the RC components of the parallel "T", to enable this cancellation, provide algebraic equations relating the RC components to the equation parameters, (CT), w_n, $(CT)_{(ld)}$, $(CT)_{(lg)}$, ζ_n, and ζ_d. Where **E** is the RMS value of signal voltage the input voltage may be written as

$$e_{(in)} = \frac{E}{2}[\cos(w_o + w_d)\,t + \cos(w_o - w_d)\,t] \qquad (7)$$

Let $(w_o + w_d)$ be defined as the upper side band and $(w_o - w_d)$ be the lower side band. With the above input it can be shown [2, 3] that the output signal voltage of the parallel "T" can be resolved into two separate sinusoidal suppressed carrier envelopes which are in exact quadrature with one another.

$$e_{(out)} = \frac{E}{2}[A_1 \cos(w_d t + \phi_d)\cos(w_o t + \phi_o) + A_2 \sin(w_d t + \phi_d)\sin(w_o t + \phi_o)] \qquad (8)$$

Sobczyk [3] calls the first term the signal envelope and the second term the quadrature envelope.

$A_1 \equiv$ the sum of the amplitude of the frequency responses of the lower and upper side bands.

$A_2 \equiv$ the difference of the amplitude of the frequency responses of the side bands.

$\phi_d \equiv$ the phase shift associated with the modulating voltage, and is equal to one half the difference in phase angles of the frequency responce of the two side bands.

$\phi_o \equiv$ the phase shift associated with the carrier voltage, and is equal to one half the sum of the phase angles of the frequency response of the two side bands.

Equation (8) neglects the proportional term generated by the parallel "T", as this term is merely a fractional transmission of the input

signal and is not frequency sensitive[2].

Now a sketch of the frequency response of the ideal frequency function, equation (2), is as shown in Fig. 3-1, and that of the actual frequency function, equation (6), in Fig. 3-2. The actual performance function of the parallel "T" is a good approximation to the ideal performance function as long as $w_d << w_o$ [3]. In most practical circuitry the spectrum of significant w_d usually extends the side bands only a short distance from w_o justifying the approximation. With equation (8) in mind and the carrier frequency of the input signal equal to the tuned frequency, w_o, of the parallel "T", it can be shown that the output signal consists only of the signal envelope and has the form

$$e_{(out)} = [E \cos w_d t + \frac{E}{2} A_1 \cos (w_d t + 90^o)] \cos w_o t$$

$$= [E \cos w_d t + E (CT)_{(ld)} w_d \cos (w_d t + 90^o)] \cos w_o t$$

$$= [E \cos w_d t + E (CT)_{(ld)} w_d (-\sin w_d t)] \cos w_o t$$

$$= [e(t) + (CT)_{(ld)} \frac{de(t)}{dt}] \cos w_o t .$$

The magnitude of the response, or output signal voltage, can be seen to increase linearly with increase of modulation frequency, w_d. Beyond a certain frequency the denominator of the actual frequency function (6) is no longer negligible and the curve (see Figs. 3-2 and B-4) flairs out.

Consider now the situation where the carrier frequency, w_c, of the input signal does not equal the tuned frequency w_o, of the signal modifier. Refer to Fig. 3-3a where the carrier frequency, w_c, has shifted an amount $D=|w_c - w_o|$, and the frequency of the modulation, w_d, is varied through its range; the upper limit being where the actual response of the parallel "T" ceases to approximate the ideal derivative characteristic. Here w_d is defined as $(w - w_c)$. Attura[2] demonstrates that as w_d increases, the amplitude of the quadrature envelope, Q, increases as a function of w_d. At the same time the amplitude of the signal envelope, S, remains constant, a function of D. As w_d passes through D, the two envelopes exchange functions.

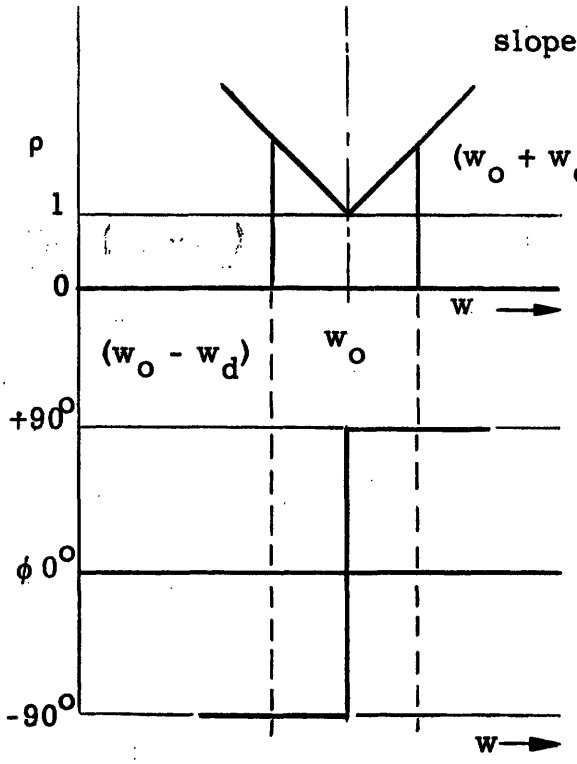

$[FF]_{(sm)} = 1 + (CT)_{(ld)}\, j\, (w - w_o)$

$w_d = w - w_o \equiv$ frequency of modulating voltage.

$(CT)_{(ld)} \equiv$ derivative time constant.

$\rho \equiv$ magnitude of $[FF]_{(sm)}$

$\phi \equiv$ argument of $[FF]_{(sm)}$

w_o tuned frequency of the signal modifier

Fig. 3-1 Sketch of the Frequency Function Characteristics of the Ideal Signal Modifier.

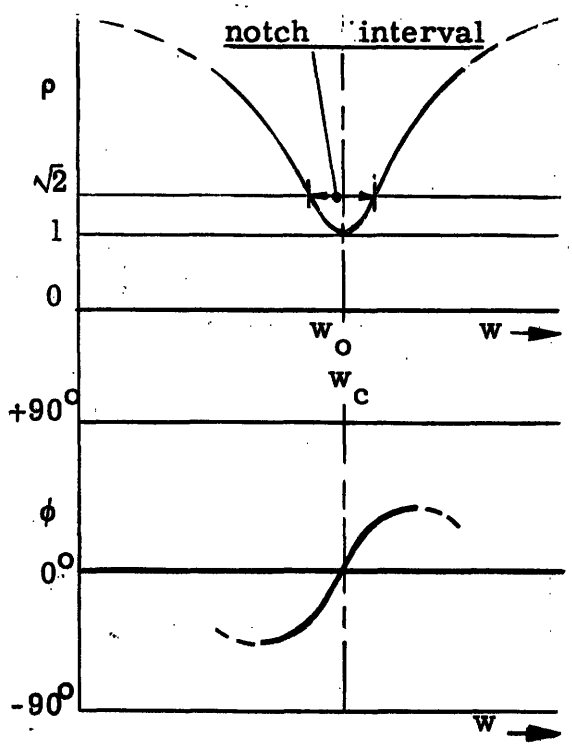

$$[FF]_{(sm)} = \frac{1 + (CT)_{(ld)}\, j\, (w - w_c)}{1 + (CT)_{(lg)}\, j\, (w - w_c)}$$

$(CT)_{(ld)} \equiv$ derivative time constant

$(CT)_{(lg)} \equiv$ integral time constant

$\rho \equiv$ magnitude of $[FF]_{(sm)}$

$\phi \equiv$ argument of $[FF]_{(sm)}$

$w_o \equiv$ tuned frequency of the signal modifier.

Fig. 3-2 Sketch of the Frequency Function Characteristics of the Actual Signal Modifier (Parallel "T")

with S increasing in magnitude with w_d; and Q remaining constant, a function of D.

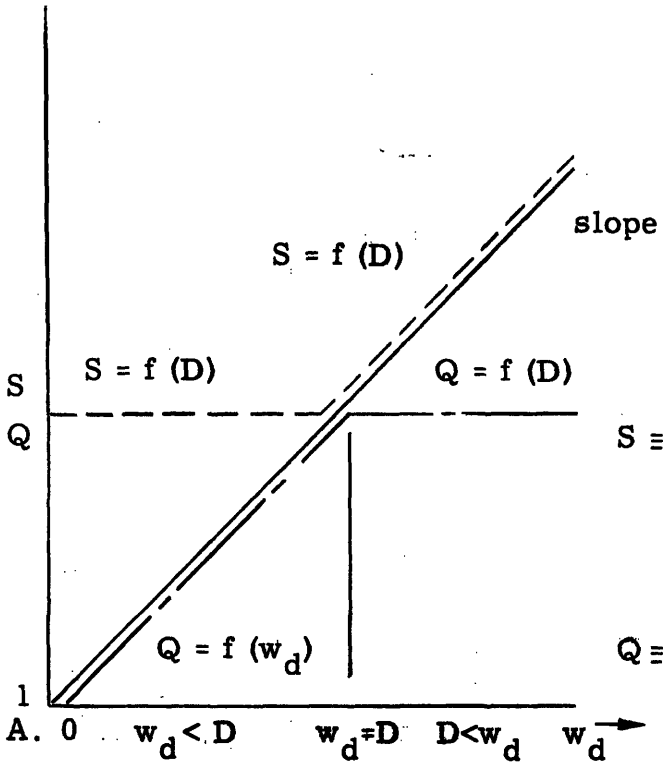

S ≡ magnitude of signal envelope

Q ≡ magnitude of quadrature envelope

D ≡ $|w_c - w_o|$; the absolute magnitude of difference between carrier frequency and tuned frequency of signal modifiers.

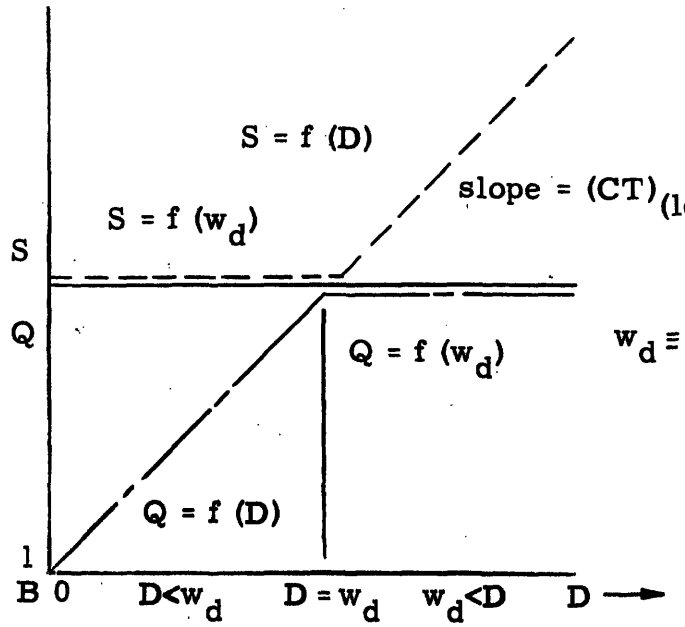

$w_d \equiv |w - w_c|$; the frequency of the modulating signal

Fig. 3-3a&b. Sketch of the Envelope Magnitudes of the Output Voltage, $e_{(out)}$, vs. Frequency of Modulation, w_d, in A and the Magnitude of Carrier Frequency Shift, D, in B.

Fig. 3-3b shows the relation of envelope magnitudes for a constant w_d and a varying D. Attura[2] further demonstrates that the envelope whose amplitude is a function of w_d is modulated by cos $(w_d + 90^o)$. The other envelope whose amplitude is a function of $D = |w_c - w_o|$ is modulated by sin $(w_d + 90^o)$. Thus any phase sensitive actuator could easily pass the preferred cosine phase and reject the unwanted sine phase. Any unbalance in the phase sensitivity of the actuator would, of course, reduce the transmission of the desired envelope and pass some of the unwanted envelope. This would consequently reduce the amount of the derivative component and distort the signal at the same time. Figs. 3-4 through 3-6 show the complete suppression of the quadrature envelope, Q, for $w_c = w_o$, the tuned frequency of the signal modifier. In Fig. 3-4a note the "noise" in the signal. This is due to the fact that at low modulator frequencies, w_d, the signal amplitude level is close to the region of atmospheric "pick up" and spurious signals originating in the synchros of the signal generator. Figs. 3-7 through 3-12 show, for a constant $D = |w_c - w_o|$, the build up of the quadrature envelope, Q, and then the signal envelope, S, as the modulation frequency, w_d, increases and passes through D. Figs. 3-13 through 3-21 show the build up of Q and then S, as D increases, for constant values of w_d.

3.3 In the experimental set up, Fig. A-5, the same means of signal geration was employed as the set up for the type I modifier in chapter 2. An audio oscillator was used to provide variable carrier frequency, w_c. Phase was measured as before with the calibrated rotor of a control transformer device[5]. The phase pattern, however, was different in that a modulated signal was beating against a modulated signal (see Figs. 3-4 through 3-30). The patterns, for the most, appeared as contracting and expanding ellipses, when the beating signal was in phase with the output modified signal. These ellipses appeared distorted when the signals were not in phase indicating incorrect measurement. It was found that as w_c shifted further from w_o, and as w_d increased to greater values (50 radians per second and greater), the pattern became exceedingly difficult to interpret. All sorts of weird configurations appeared (see Fig. 3-9b). However, several methods[2, 4] of phase measurement were employed with less success

than the one described. These included use of a commercial phase meter and a double beam cathode ray oscilloscope. Envelope magnitudes were measured by counting squares on the grid face of the cathode ray oscilloscope. The Heathkit voltage calibrator used in chapter 2 would not function properly with change in carrier frequency of the input signal. All elements were properly grounded to reduce pick up noise. In making up the modifier and filters the series resistances and shunt condensers were combined with variable elements (see Fig. A-6). This faciliated the tuning [4] of each network to its designed frequency. Precision RC components were not and generally are not available and therefore not used. At this the parallel "T" was tuned to within 1 cps of 60 cps. This proved not to be critical in determination of the frequency response characteristics.

3.4 In order to obtain reasonable amplitude variation within the available range of modualtion frequency, it was necessary to select a relative large derivative time constant, $(CT)_{(ld)}$, resulting in a narrow rejection band and a narrow notch interval, NI. Sobczyk[3] defines the notch interval as the length of the frequency interval between the points at which the ouput magnitude is $[2]^{1/2}$ times the minimum output (see Fig. 3-2). A notch interval of 2.0 cps. was selected giving a derivative time constant of

$$(CT)_{(ld)} = \frac{2}{2\pi \ NI(cps)} = .16 \text{ secs.}$$

The integral time constant, $(CT)_{(lg)}$, is related to $(CT)_{(ld)}$ by the product of $(CT)_{(ld)}$ and the amplitude gain of the network[3]. For the parallel "T" designed (without smoothing filters) the gain is calculated to be .008 [3]. Therefore $(CT)_{(lg)} = .008\ (CT)_{(ld)} = .00128$ secs. Thus the breakpoint for the numerator factor of equation (6) would plot at $\frac{1}{.16} = 6.28$ radians/ sec. The breakpoint for the denominator factor would plot at $\frac{1}{.00128} = 780$ radians/ sec., or about two lorus[13] further out on the frequency scale. Plotting first order theoretical frequency response curves[13] at these breakpoints indicates the following: (a) A maximum phase lead of about 85° at a modulation frequency, w_d, of about 6 cps. (b) A maximum amplitude gain of 42db at about 1000 cps. (-42 db is the design gain figure at 60 cps). (c) Ideal phase

response up to w_d = 4 cps. (d) Ideal amplitude response up to w_d = 40 cps. neglecting effect of $(\frac{w+w_o}{2w})$ which is necessary for first order approximation.

Next came the problem of filters to smooth out signal noise generated in the signal generator synchros [3, 5] and network itself [7] (see Figs. 3-22 through 3-39). Two low pass RC filters were put between the signal generator and parallel "T". The break points were selected at 60 cps and 120 cps. RC values were chosen such that the output impedance was less than the input impedance of the parallel "T" by a factor of about 10. The adjustment of impedance levels precluded the necessity of using isolation networks such as transformers or cathode followers. The input impedance level of the low pass filters was reasonably high to prevent loading down of the control transfomer. The rotor of the control transformer had an open circuit impedance of about 550 ohms. Assuming negligible loading effects the carrier phase lag due to the filters at 60 cps was about 60^o. This was substantially verified by actual phase measurements across the filter. Examination of the carrier wave using the smoothing filters in conjunction with the parallel "T" (See Fig. 3-33) gave evidence of a considerably less noisy signal. Evident also was a large amplitude third harmonic (180 cps). To suppress this harmonic another parallel "T" network was put in (see Fig. A-6). Its impedance level was about 10 times the output impedance of the signal modifier parallel "T". The resulting carrier wave is as shown in Fig. 3-34. The cleanliness of the wave was more evident with w_c shifted off the tuned frequency of w_o = 60 cps (see Fig. 3-37). For a full rejection band parallel "T" ($(CT)_{(1d)} = \infty$), the limitation of low complete the rejection at the tuned frequency is "pick up" and spurious signals due to stray inductance and capacitance in the network componets[4]. With all filters connected in series frequency response data were taken and plotted (see Figs. B-4 to B-7).

The amplitude response (Fig B-5) does show that the modifier closely approximates the ideal characteristics of equation (1). The breakpoint is one half cps lower than the designed breakpoint of 1 cps. This is possible due to loading effect, however small, of the filters. It was not possible to verify the upper limit of amplitude approximation,

as modulation frequency, w_d, was available only to 11 cps. The amplitude response (Fig. B-4) for carrier frequency shows the narrow notch of the actual modifier with filters. The notch interval, NI, is about 1 1/2 cps as compared to the design NI of 2 cps. The response data for both amplitude and phase were not too reliable at the low modulation frequencies due to the low signal magnitude level at these frequencies. Further inspection of Fig. B-4 shows that the linear amplitude approximation of the ideal modifier falls off at about 70 cps. This indicates that a carrier shift of about 16% is allowable before the desired proportional plus derivative characteristic is no longer obtained. This allowable percentage is amplitude wise only. The phase data of Figs. B-6 and B-7 show that for a carrier frequency of 60 cps a maximum lead of 84 degrees is obtained at a modulation frequency of about 4 cps. For a numerator first order factor with a breakpoint at .5 cps, the maximum phase lead obtainable with the parallel "T" is 80 degrees at about 5 cps. From a study of both phase and amplitude curves it is believed that the addition of the smoothing filters shifted the tuned frequency of the modifier to about 59.5 cps. Even with this apparent shift of the tuned frequency the approximation to the ideal characteristics is good out to a modulation frequency of about 3 cps. As carrier frequency, w_c, shifts away from the tuned frequency, w_o, the phase lead drops off rapidly. For w_c equal to 62 cps and higher the network develops phase lag. This is due to the fact that the difference between the phase angles associated with the side bands becomes negative, when the sum of the carrier frequency shift, D, and w_d becomes greater than 4 cps - the frequency of maximum phase lead. Because of the method used in measuring phase, the phase data of Figs. B-6 and B-7 represent the phase of the envelope (signal or quadrature) that had the largest amplitude for the given combination of w_c and w_d.

3.5 The conclusions drawn from the mathematical theory and experimental data are as follows:

(a) The parallel "T" performance function represented by equations (5a) and (5b) closely approximate the ideal proportional plus derivative characteristic. The network does not differentiate within frequency limits of a charge in carrier, w_c, or modulation frequency,

w_d. Within a carrier frequency shift of 16% the first order amplitude response associated with equation (5a) approximates the ideal. For the network used in the experiment a sum of modulation frequency, w_d, and carrier frequency shift, D, of up to 4 cps can be tolerated. For systems involving high values of w_d where the approximation $\frac{w + w_o}{2w} \approx 1$ is not valid the simplifying equation (6) cannot be used and equation (5b) must be employed. In this respect it is advantageous to utilize the second order frequency response curves of reference [13] in analysis. Equation (5b) requires no simplifying assumptions.

(b) If the output of the parallel "T" is passed through a phase sensitive device, the unwanted envelope proportional to change of carrier frequency, D, can be suppressed[2]. As long as the reference phase of the device remains in phase with the unwanted envelope, any degree of carrier frequency shift will not reduce or distort the desired envelope. The desired envelope is the envelope whose amplitude is a function of the modulation frequency, and it is the envelope actuating the device. The amount[2] of distortion or noise in the output of a phase sensitive device is proportional to the sin of the angle between the phase of the unwanted envelope and the phase of the reference voltage.

(c) A more serious limitation caused by the presence of the unwanted or quadrature envelope of the signal modifier output is the instantaneous voltage level of the sum of the signal and quadrature amplitudes. This would tend to drive other network devices (motors, amplifiers, etc.) into non-linear regions of saturation.

(d) The selection of the derivative time constant, $(CT)_{(1d)}$ establishes the lower limit of modulation frequency, w_d, where useful phase lead may be obtained (see Figs. B-6 and B-7). If a small $(CT)_{(1d)}$ is necessary with resulting wide notch width, and low frequency phase shift important, a type II chopper RC modifier should be used.

(e) Despite the complete suppression of the quadrature envelope of the modifier output voltage, when the carrier frequency equals the tuned frequency of the modifier, there is present some signal distortion at low modulation frequencies. This comes from the low magnitude level of the signal voltage close to the null of the parallel "T".

(f) Phase data at high and low modulation frequencies are not too reliable due to the difficulty in interpreting the pattern. An easier method for obtaining more reliable measurements would be provide a phase detector on the output of the signal modifier. Thus a demodulated signal could be measured against the modulated signal input. As shown in the photographs of chapter 4, this is by far the better method for measuring phase.

(g) The design of a parallel "T" network must be a compromise between the network gain (equal to the ratio of the integral and derivative time constants) and the type of phase modification desired. More phase lead mus accompany more magnitude attenuation. This means a more narrow notch width. However, with a more narrow notch greater carrier frequency shift ean be tolerated.

(h) Figs. B-8 and B-9 show the theoretical response curves for the first order approximation equation (6) of the parallel "T" . These curves were drawn with the numerator break point at .5 cps and denominator break point at 63 cps for a gain figure of .008.

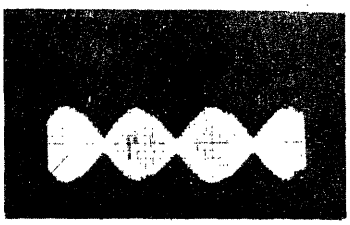

Fig. 3-4A Signal Modifier (With Filters) Output for $w_c = w_o = 377$ Rads. /sec and $w_d = 6.35$ Rads. /sec.

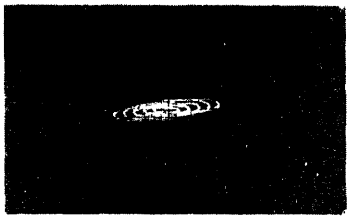

Fig. 3-4B Signal Modifier Phase Pattern.

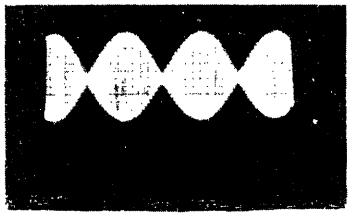

Fig. 3-4C Signal Generator Output.

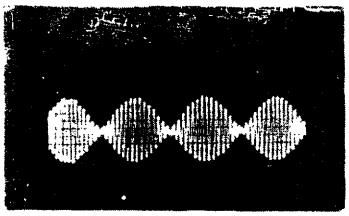

Fig. 3-5A Signal Modifier (With Filters) for $w_c = w_o = 377$ Rads. /sec and $w_d = 12.03$ Rads. /sec.

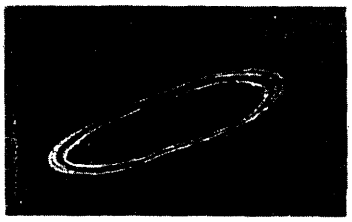

Fig. 3-5B Signal Modifier Phase Pattern.

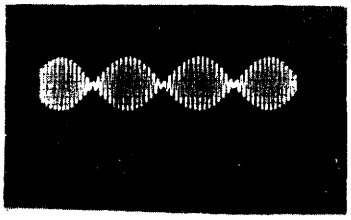

Fig. 3-5C Signal Generator Output.

Signal Modifier and Corresponding Signal Generator Output Wave Forms

Fig. 3-6A Signal Modifier (With Filters) Output for $w_c = w_o = 377$ Rads./sec and $w_d = 45.9$ Rads./sec.

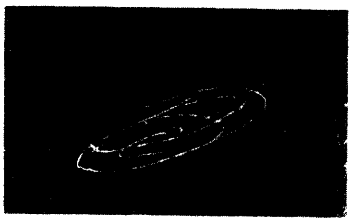

Fig. 3-6B Signal Modifier Phase Pattern.

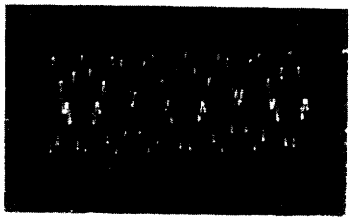

Fig. 3-6C Signal Generator Output.

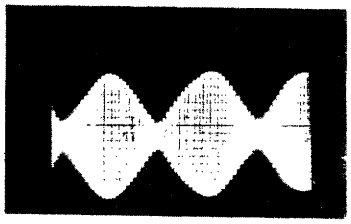

Fig. 3-7A Signal Modifier (With Filters) Output for $w_c = 345$ Rads./sec and $w_d = 6.35$ Rads./sec.

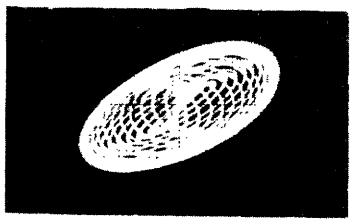

Fig. 3-7B Signal Modifier Phase Pattern.

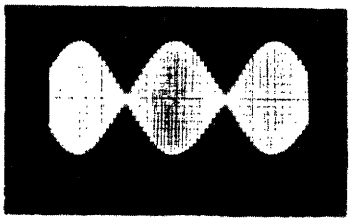

Fig. 3-7C Signal Generator Output.

Signal Modifier and Corresponding Signal Generator Output Wave Forms.

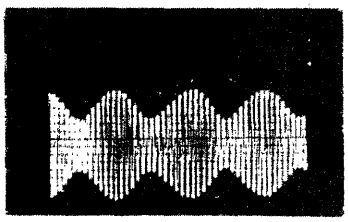

Fig. 3-8A Signal Modifier (With Filters) Output for w_c = 345 Rads. /sec and w_d = 12.03 Rads. /sec.

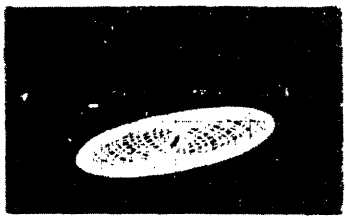

Fig. 3-8B Signal Modifier Phase Pattern.

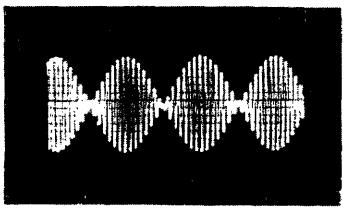

Fig. 3-8C Signal Generator Output.

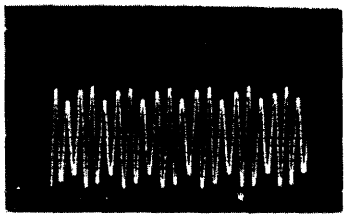

Fig. 3-9A Signal Modifier (With Filters) Output for w_c = 345 Rads. /sec and w_d = 45.9 Rads. /sec.

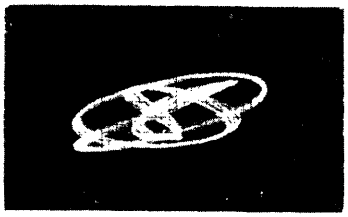

Fig. 3-9B Signal Modifier Phase Pattern.

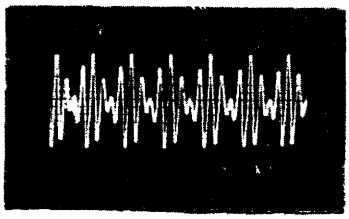

Fig. 3-9C Signal Generator Output.

Signal Modifier and Corresponding Signal Generator Output Wave Forms.

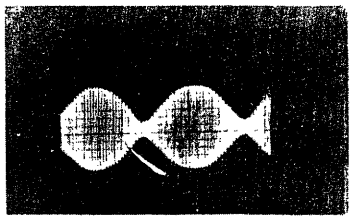

Fig. 3-10A Signal Modifier (With Filters) Output for w_c = 408 Rads./sec and w_d = 6.35 Rads./sec.

Fig. 3-10B Signal Modifier Phase Pattern.

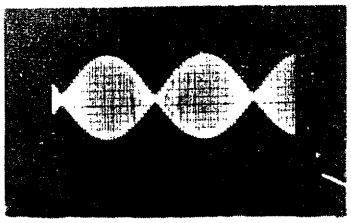

Fig. 3-10C Signal Generator Output.

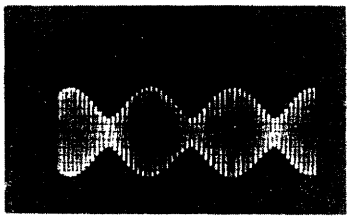

Fig. 3-11A Signal Modifier (With Filters) Output for w_c = 408 Rads./sec and w_d = 12.03 Rads./sec.

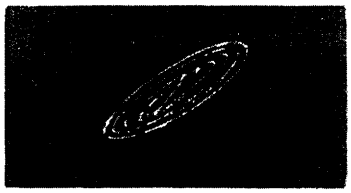

Fig. 3-11B Signal Modifier Phase Pattern.

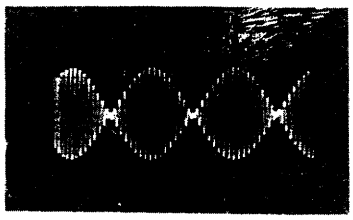

Fig. 3-11C Signal Generator Output.

Signal Modifier and Corresponding Signal Generator Output Wave Forms.

Fig. 3-12A Signal Modifier (With Filters) Output for w_c = 408 Rads. /sec and w_d = 45.9 Rads. /sec.

Fig. 3-12B Signal Modifier Phase Pattern.

Fig. 3-12C Signal Generator Output.

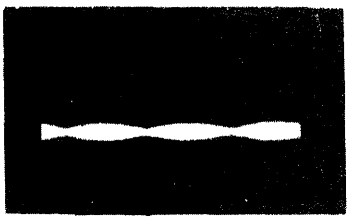

Fig. 3-13 Signal Modifier (With Filters) Output for w_c = 377 Rads/sec and w_d = 6.35 Rads. / sec.

Fig. 3-14 Signal Modifier (With Filters) Output for w_c = 383.3 Rads. /sec and w_d = 6.35 Rads. /sec.

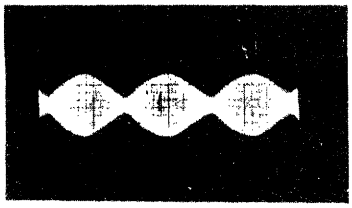

Fig. 3-15 Signal Modifier (With Filters) Output for w_c = 408 Rads. /sec and w_d = 6.35 Rads. /sec.

Various Signal Modifier Output Wave Forms

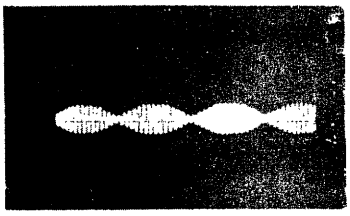

Fig. 3-16 Signal Modifier (With Filters) Output for w_c = 377 Rads./sec and w_d = 12.03 Rads./sec.

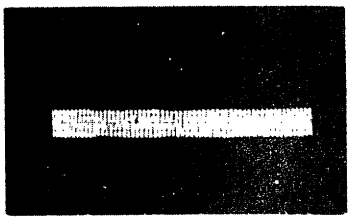

Fig. 3-17 Signal Modifier (With Filters) Output for w_c = 389.4 Rads./sec and w_d = 12.03 Rads./sec.

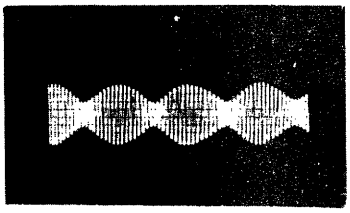

Fig. 3-18 Signal Modifier (With Filters) Output for w_c = 408 Rads./sec and w_d = 12.03 Rads./sec.

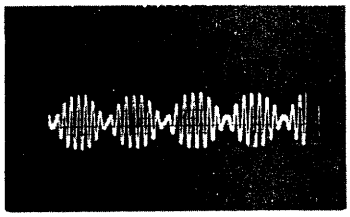

Fig. 3-19 Signal Modifier (With Filters) Output for w_c = 377 Rads./sec and w_d = 24.7 Rads./sec.

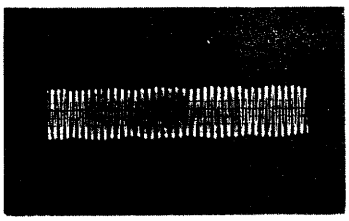

Fig. 3-20 Signal Modifier (With Filters) Output for w_c = 402 Rads./sec and w_d = 24.7 Rads./sec.

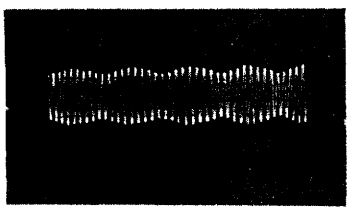

Fig. 3-21 Signal Modifier (With Filters) Output for w_c = 408 Rads./sec and w_d = 24.7 Rads./sec.

Signal Modifier Output Wave Forms for Various Frequency Values

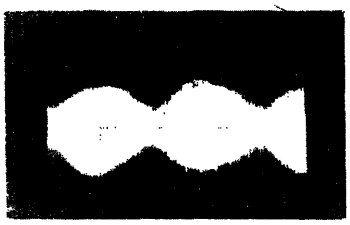

Fig. 3-22A Signal Modifier (Without Filters) Output for w_c = 377 Rads. / sec and w_d = 6.35 Rads. / sec.

Fig. 3-22B Signal Modifier Phase Pattern.

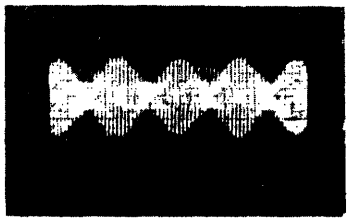

Fig. 3-23A Signal Modifier (Without Filters) Output for w_c = 377 Rad/sec and w_d = 12.03 Rads. /sec.

Fig. 3-23B Signal Modifier Phase Pattern.

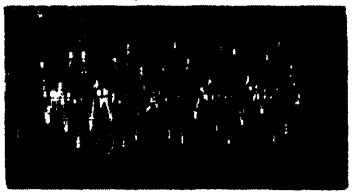

Fig. 3-24A Signal Modifier (Without Filters) Output for w_c = 377 Rads. /sec w_d = 45.9 Rads. /sec

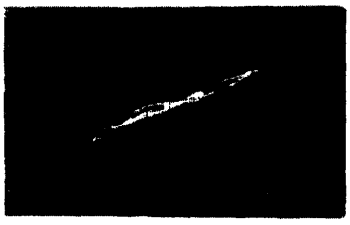

Fig. 3-24B Signal Modifier Phase Pattern.

Signal Modifier (Without Filters) Output Wave Forms

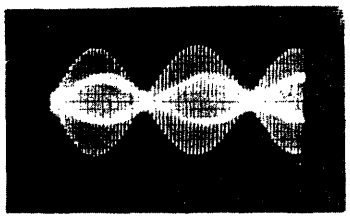

Fig. 3-25A Signal Modifier (Without Filters) Output for w_c = 345 Rads./sec and w_d = 6.35 Rads./sec.

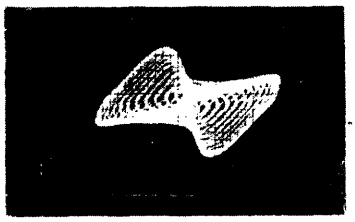

Fig. 3-25B Signal Modifier Phase Pattern.

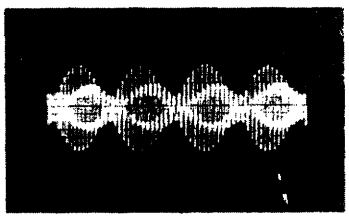

Fig. 3-26A Signal Modifier (Without Filters) Output for w_c = 345 Rads./sec and w_d = 12.03 Rads./sec.

Fig. 3-26B Signal Modifier Phase Pattern.

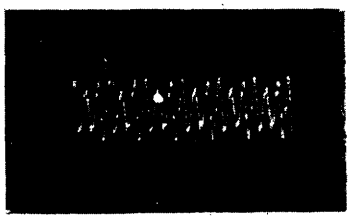

Fig. 3-27A Signal Modifier (Without Filters) Output for w_c = 345 Rads./sec and w_d = 45.9 Rads./sec.

Fig. 3-27B Signal Modifier Phase Pattern.

Signal Modifier (Without Filters) Output Wave Forms.

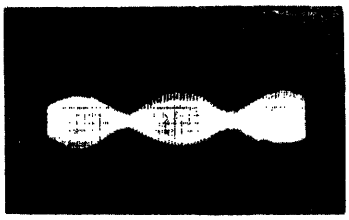

Fig. 3-28A Signal Modifier (Without Filters) Output for w_c = 408 Rads./sec and w_d = 6.35 Rads./sec.

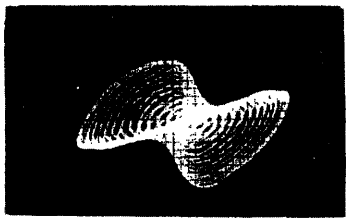

Fig. 3-28B Signal Modifier Phase Pattern.

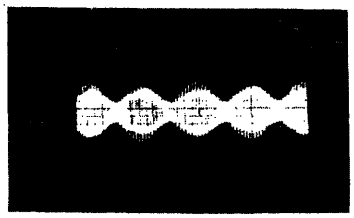

Fig. 3-29A Signal Modifier (Without Filters) Output for w_c = 408 Rads./sec and w_d = 12.03 Rads./sec.

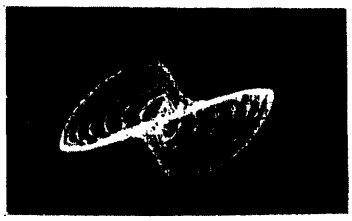

Fig. 3-29B Signal Modifier Phase Pattern.

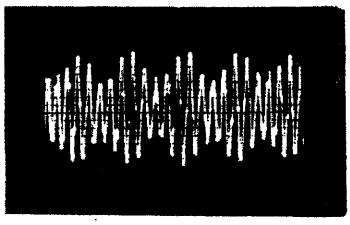

Fig. 3-30A Signal Modifier (Without Filters) Output for w_c = 408 Rads./sec and w_d = 45.9 Rads./sec.

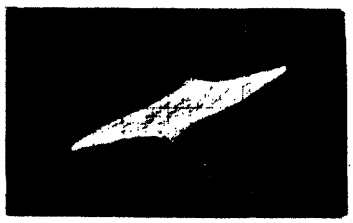

Fig. 3-30B Signal Modifier Phase Pattern.

Signal Modifier (Without Filters) Output Wave Forms.

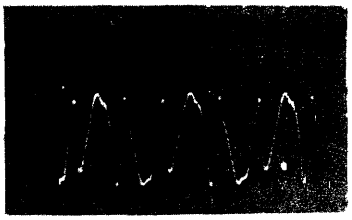

Fig. 3-31A Signal Modifier Carrier Output (Without Filters) in Phase Component for w_c = 377 Rads./sec and w_d = 0.

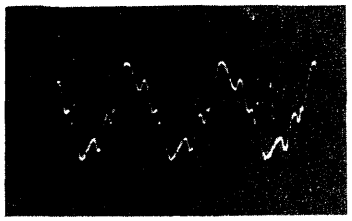

Fig. 3-31B The Quadrature Phase Component for Output Signal.

Fig. 3-32A Signal Modifier in Phase Component of Carrier Output with 180 cps Filter and w_c = 377 Rads./sec and w_d = 0.

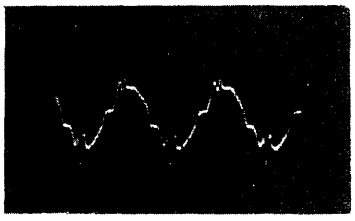

Fig. 3-32B The Quadrature Phase Component for the Output Signal.

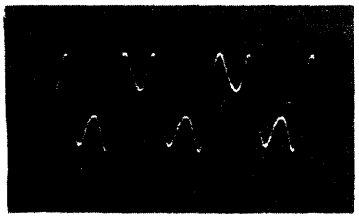

Fig. 3-33A Signal Modifier in Phase Component of Carrier Output with Low Pass Filter and w_c = 377 Rads./sec. w_d = 0.

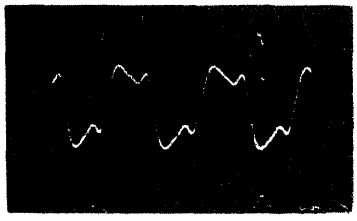

Fig. 3-33B The Quadrature Phase Component for the Output Signal.

Signal Modifier Carrier Output Wave Forms.

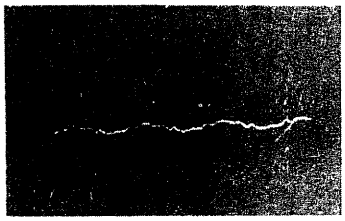

Fig. 3-34 Signal Modifier Carrier Output with all Filters for w_c = 377 Rads./sec. Gain ≈ -40db.

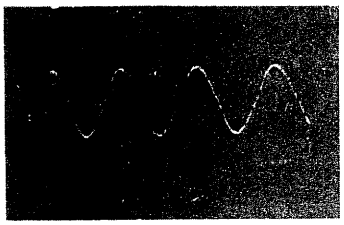

Fig. 3-35 Signal Generator Carrier Output with all Filters for w_c = 377 Rads./sec. w_d = 0. Gain ≈ - 32db.

Fig. 3-36 Carrier Generator Output at w_c = 377 Rads./sec.

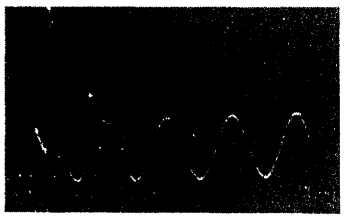

Fig. 3-37 Signal Modifier Carrier Output with all Filters for w_c = 345 or 408 Rads./sec. Gain ≈ -40db.

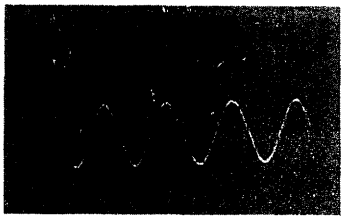

Fig. 3-38 Signal Generator Carrier Output with all Filters for w_c = 345 and 408 Rads./sec. Gain ≈ - 26db.

Fig. 3-39 Carrier Generator Output at w_c = 345 or 408 Rads./sec.

Signal Modifier (With Filters) Carrier Wave Forms.

CHAPTER 4

THE CHOPPER AS A TYPE II A.C. SIGNAL MODIFIER

4.1 The alternating current rate circuit analysis by Donovan[8] may be simplified by assuming a solution and developing the equation for the circuit parameters. If it is assumed that the transfer function of the circuit is $\frac{CT\ P}{CT\ P+1}$, the analysis of the response of the circuit for a step input is as follows:

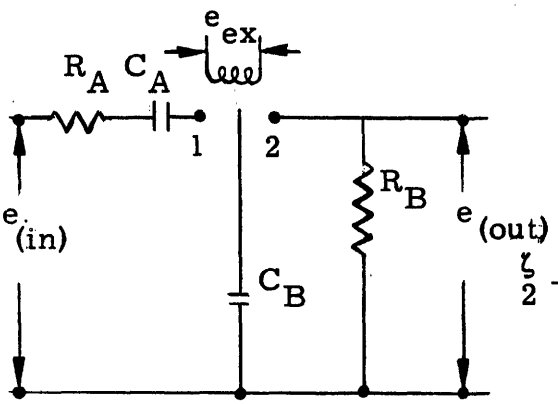

Fig. 4-1 Chopper R.C. Network Used as a Signal Modifier.

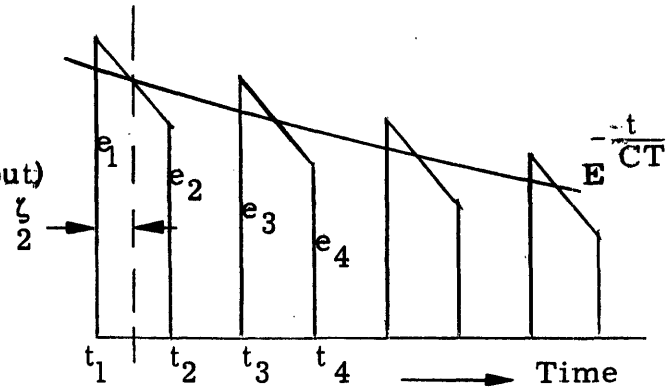

Fig. 4-2 Assumed Step Response for Figure 4-1.

Let:

e_{in} = increasing step voltage

δ = dwell time of reed on contact #2

T_n = period of reed excitation voltage (e_{ex})

K_1 = $C_A / (C_A + C_B)$

K_2 = $C_B / (C_A + C_B)$

The response of the transfer function $\frac{CT\ P}{CT\ P+1}$ to an unit increasing step voltage is the same as the response of $\frac{CT}{CT\ P+1}$ to an unit impluse of voltage. Namely, it is a decaying exponential.

4.2 Referring to Fig. 4-1 and 4-2: Assume that R_A, C_A, C_B are such that C_B is completely charged during the time that the reed is on contract #1.

$e_1, e_2, e_3, e_4,$ are output voltages

at $t_1, t_2, t_3, t_4,$ respectively.

$t_2 - t_1 = t_4 - t_3 = \delta$

$$e_1 = e_o \frac{C_A}{C_A + C_B} = K_1 e_o \tag{1}$$

$$e_2 = e_1 \epsilon^{-\frac{\delta}{R_B C_B}} = K_1 e_o \epsilon^{-\frac{\delta}{R_B C_B}} \tag{2}$$

$$e_3 = [\, e_o - (\text{Voltage on } C_{A_{[t = t_2]}}) - e_2] \frac{C_A}{C_A + C_B} + e_2 \tag{3}$$

but Voltage on $C_{A_{[t = t_2]}} = e_o \frac{C_B}{C_A + C_B} = K_2\ e_o$

$$e_3 = [\, e_o - K_2 e_o - K_1 e_o \epsilon^{-\frac{\delta}{R_B C_B}}] K_1 + K_1 e_o \epsilon^{-\frac{\delta}{R_B C_B}} \tag{4}$$

$$e_4 = e_3 \epsilon^{-\frac{\delta}{R_B C_B}} \tag{5}$$

If it is assumed that the interval $t_2 - t_1$, $t_4 - t_3$ is short enough so that the voltage decay across R_B during this interval is essentially linear. (Fig. 4-2)

Then,

$$\left(\frac{e_1 + e_2}{2}\right) \epsilon^{-\frac{T_n}{CT}} = \frac{e_3 + e_4}{2} \tag{6}$$

$$K_1 e_o \left(1 + \epsilon^{-\frac{\delta}{R_B C_B}}\right) \epsilon^{-\frac{T_n}{CT}} = e_2 \left(1 + \epsilon^{-\frac{\delta}{R_B C_B}}\right) \tag{7}$$

$$K_1 e_o \epsilon^{-\frac{T_n}{CT}} = e_2 \tag{8}$$

$$K_1 e_o \epsilon^{-\frac{T_n}{CT}} = K_1 e_o \left[1 - K_2 - K_1 \epsilon^{-\frac{\delta}{R_B C_B}} + \epsilon^{-\frac{\delta}{R_B C_B}}\right] \tag{9}$$

but $1 - K_2 = K_1$

$$\epsilon^{-\frac{T_n}{CT}} = K_1 + (1 - K_1) \epsilon^{-\frac{\delta}{R_B C_B}} + \epsilon^{-\frac{\delta}{R_B C_B}} \tag{10}$$

$$CT = -\frac{T_n}{\ln \left[K_1 + (1 - K_1) \epsilon^{-\frac{\delta}{R_B C_B}}\right]} \tag{11}$$

4.3 For the plot of Figs. B-8, 9, amplitudes were measured by counting squares on the face of the oscilloscope. Phase was measured by the method described in section 2.3. (see Figs. 4-2 to 6)

4.4 The conclusions drawn are as follows:

(a) Since this technique of signal modification delivers only one half of the modulated wave, its application may be limited.

(b) Care must be exercised in interpreting the phase response of this circuit. Since t=o must be at the instant the reed meets contact #1, i.e. condenser C_B begins to charge, there is, in addition to the lag term in the denomenator of the transfer function, a finite time delay. This constant time delay is equal to the dwell time on contact #1 plus the transit time of the reed to contact #2 plus $\frac{\delta}{2}$. The last term must be included since the derivation of the frequency response is based on an average value of the voltage at the beginning and at the end of the of

the discharge period. For a 60 cycle chopper this time is, in order of magnitude equal to .013 sec.

Fig. 4-1 Signal Modifier Output for w_d = 6.35 Rads./sec. The Oscilloscope X sweep is spread out showing Square Wave Form of the Chopped Carrier.

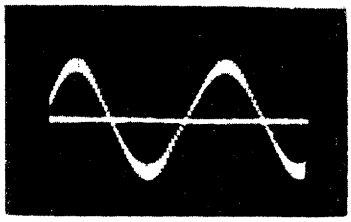

Fig. 4-2 Signal Modifier Output for w_d = 6.35 Rads./sec, and Oscilloscope X Sweep Not Spread Out.

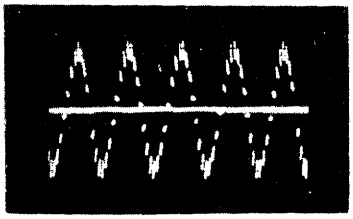

Fig. 4-3 Signal Modifier Output for w_d = 22.7 Rads./sec.

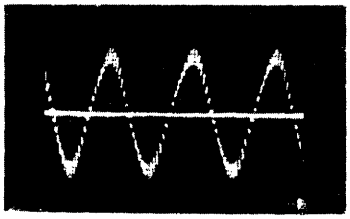

Fig. 4-4 Signal Modifier Output for w_d = 11.6 Rads./sec.

Fig. 4-5 Phase Pattern for w_d = 6.35 Rads./sec. Phase Measuring Device Reads Correct Phase with this Pattern.

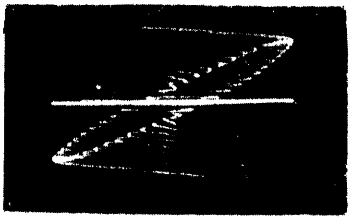

Fig. 4-6 Phase Pattern for w_d = 6.35 Rads./sec and Phase Measuring Device not Reading Correct Phase.

Type II System Using the Chopper RC Network Signal Modifier Output Wave Forms and Phase Patterns for Different Modulation Frequencies.

APPENDIX A

FUNCTIONAL AND SCHEMATIC DIAGRAMS OF EXPERIMENTAL CIRCUIT SET UPS

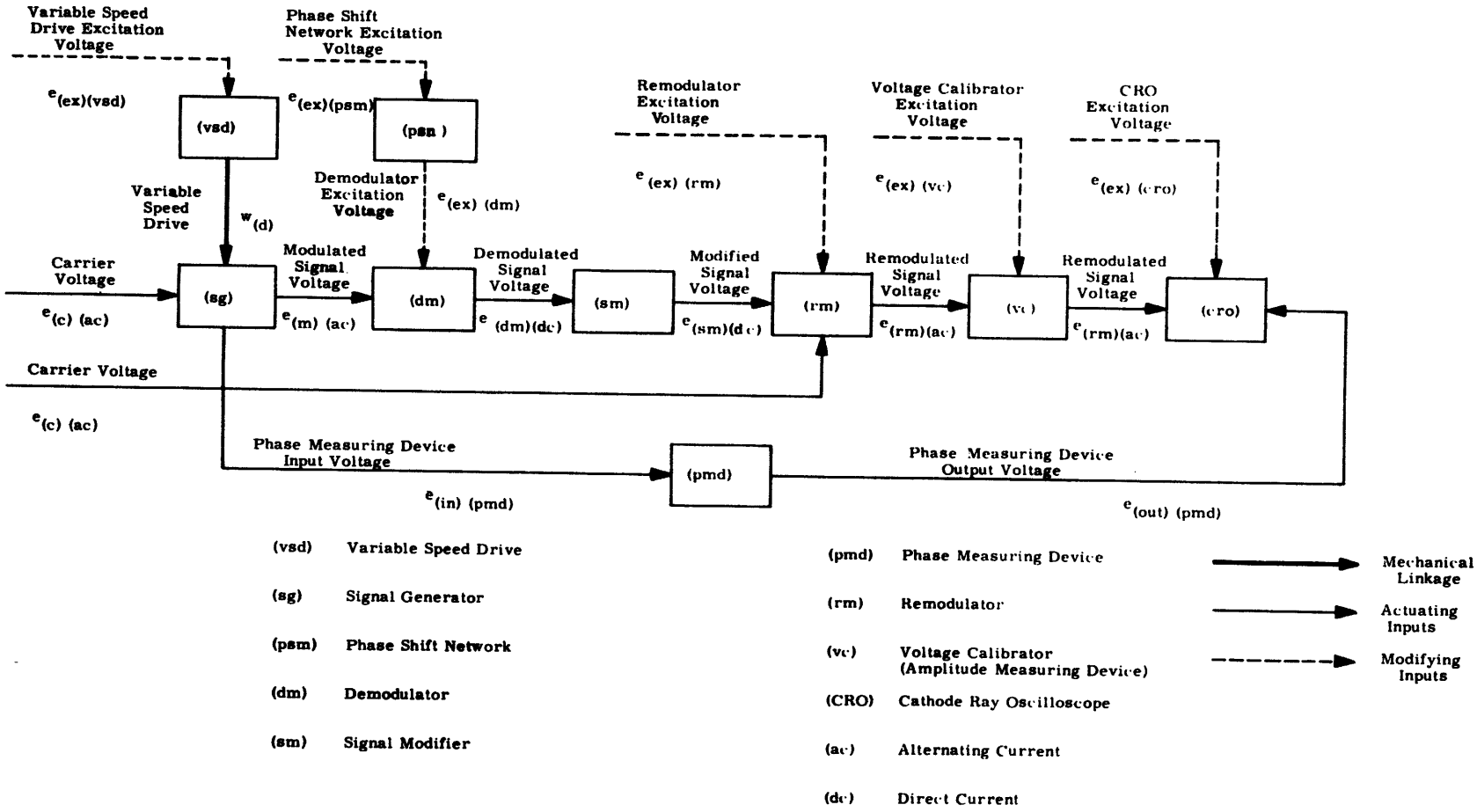

Fig. A-1 Functional Diagram for D.C. Signal Modifier Test Set Up

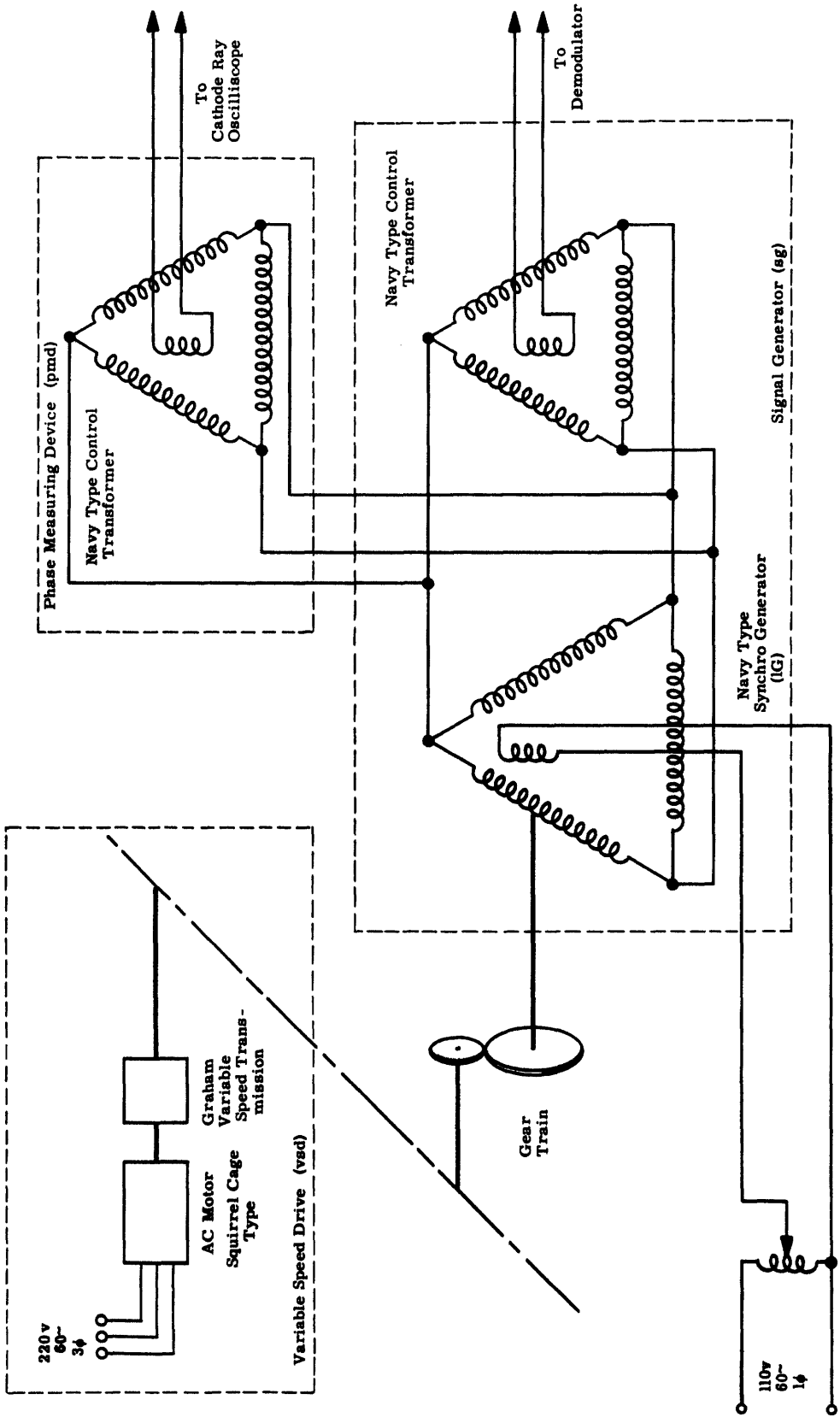

Fig. A-2 Schematic Diagram for Variable Speed Drive, Signal Generator, and Phase Measuring Device for D.C. Signal Modifier Test Set Up

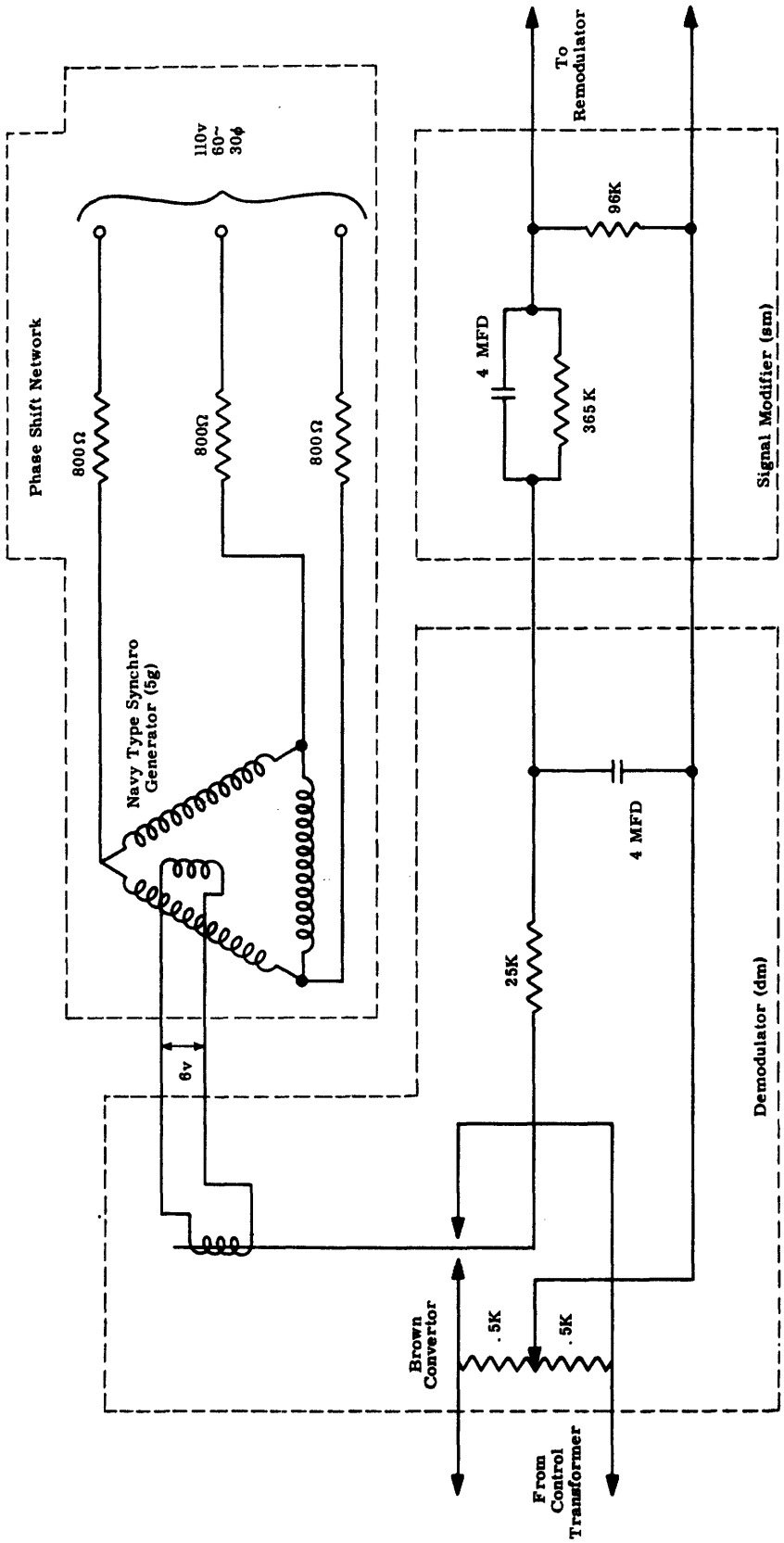

Fig. A-3 Schematic Diagram for Demodulator, Phase Shift Network, and Signal Modifier for D.C. Signal Modifier Set Up

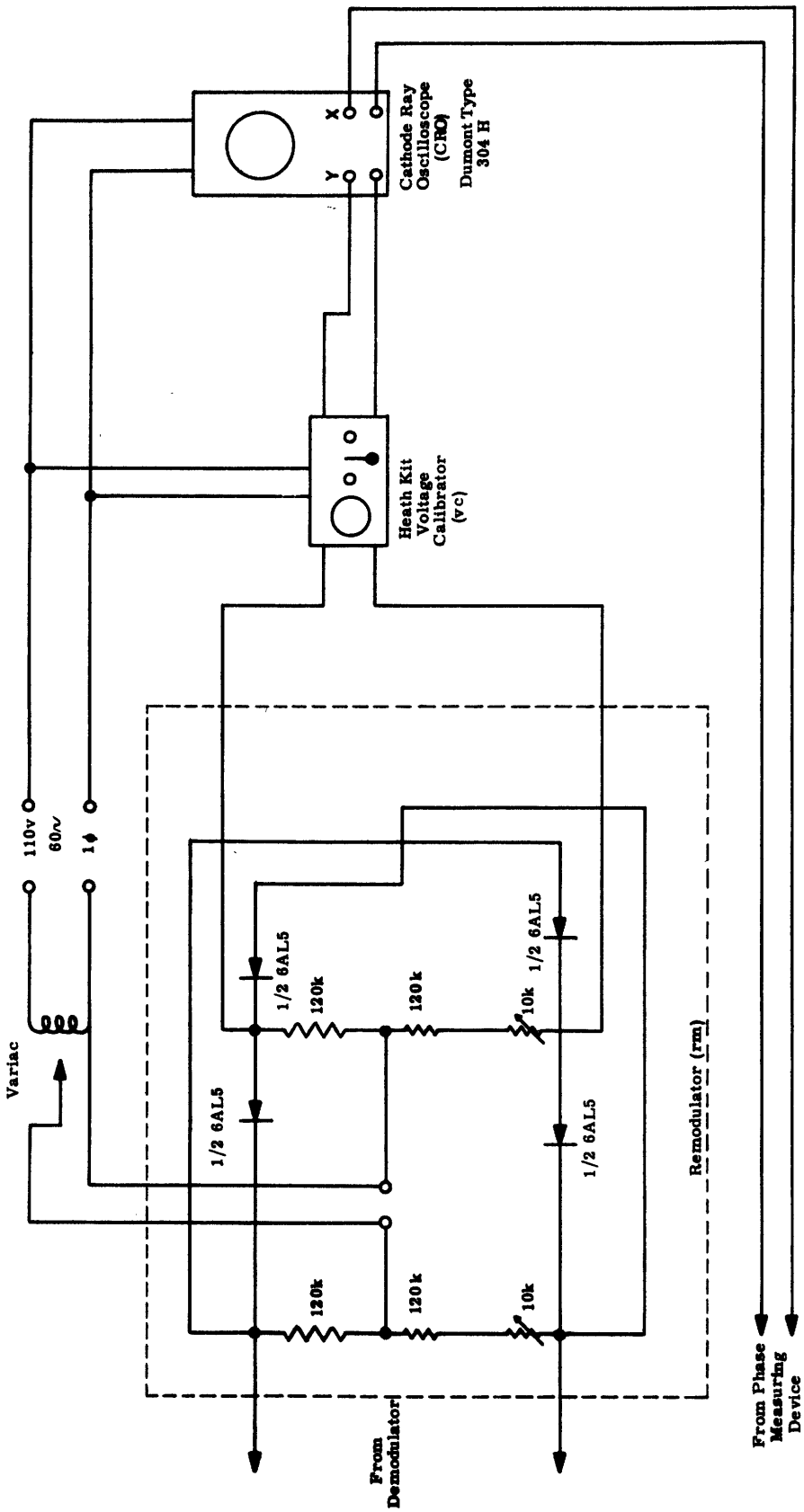

Fig. A-4 Schematic Diagram for Demodulator with Voltage Calibrator and Cathode Ray Oscilloscope for D.C. Signal Modifier Test Set Up.

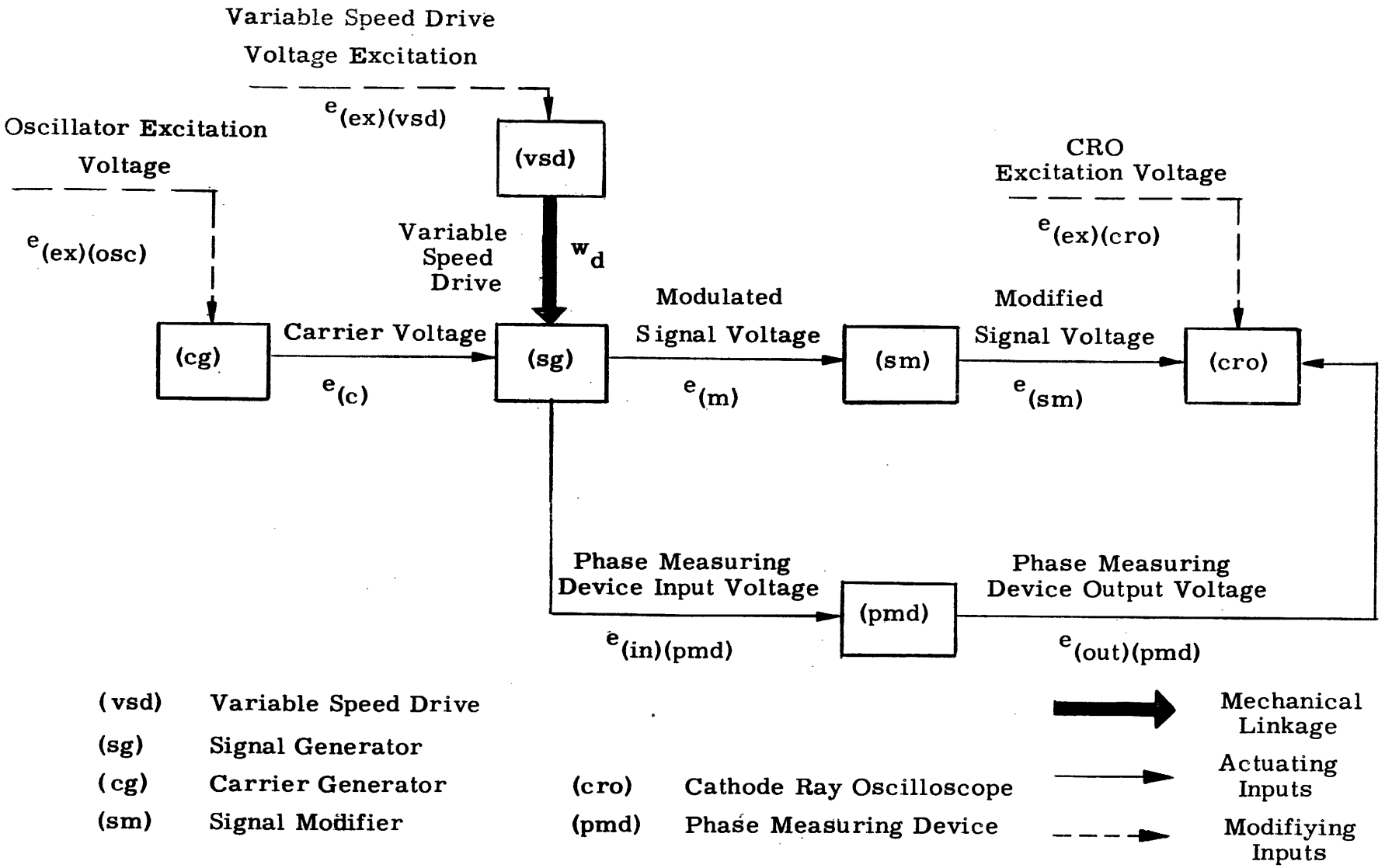

Fig. A-5 Functional Diagram for A.C. Signal Modifier (Parallel "T") Test Set Up.

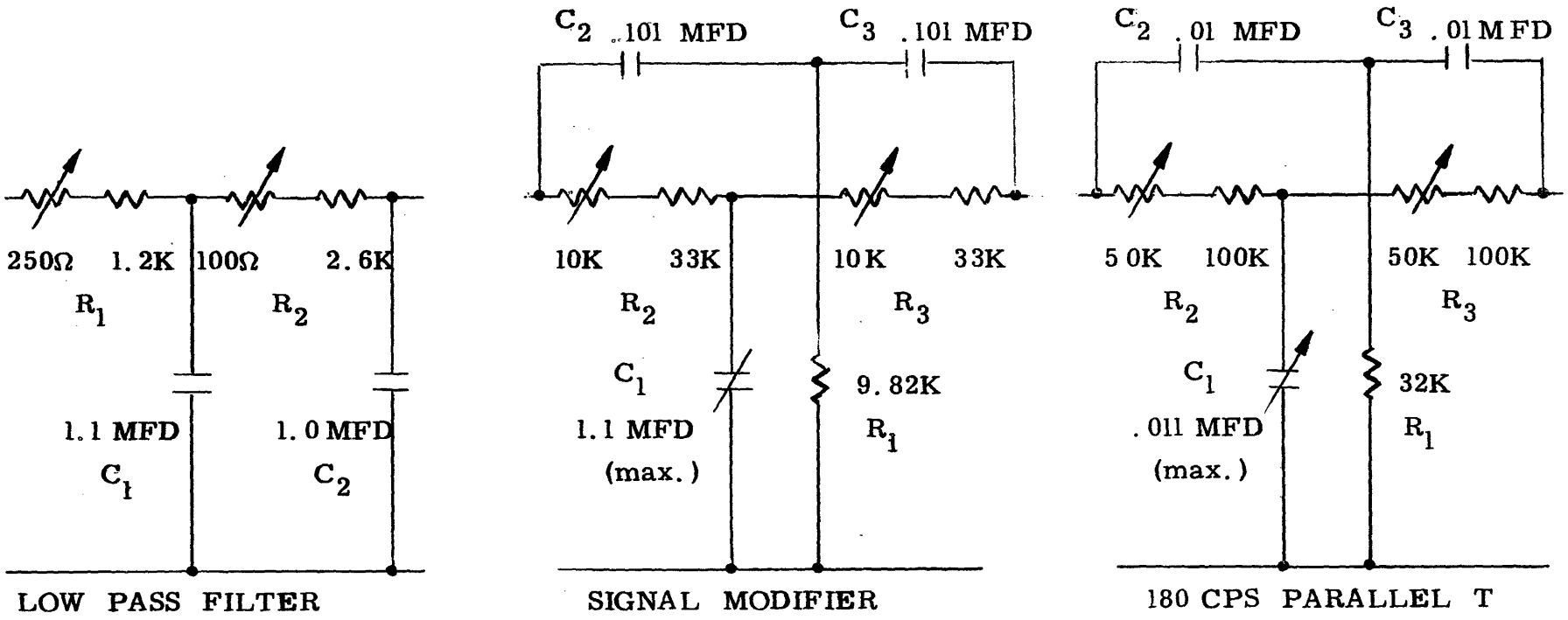

	With Filters	Without Filters	
R_1 = 1.325K	R_1 = 9.82K	R_1 = 9.82K	R_1 = 32K
R_2 = 2.65K	R_2 = 35K	R_2 = 35.8K	R_2 = 126K
C_1 = 1.0 MFD	R_3 = 39K	R_3 = 37.5K	R_3 = 126K
C_2 = 1.0 MFD	C_1 = .11 MFD	C_1 = .10 MFD	C_1 = .0103 MFD
	C_2 = .101 MFD	C_2 = .101 MFD	C_2 = .01 MFD
	C_3 = .101 MFD	C_3 = .101 MFD	C_3 = .01 MFD

Fig. A-6 Schematic Diagram for Signal Modifier with Filters for A.C. Signal Modifier Test Set Up

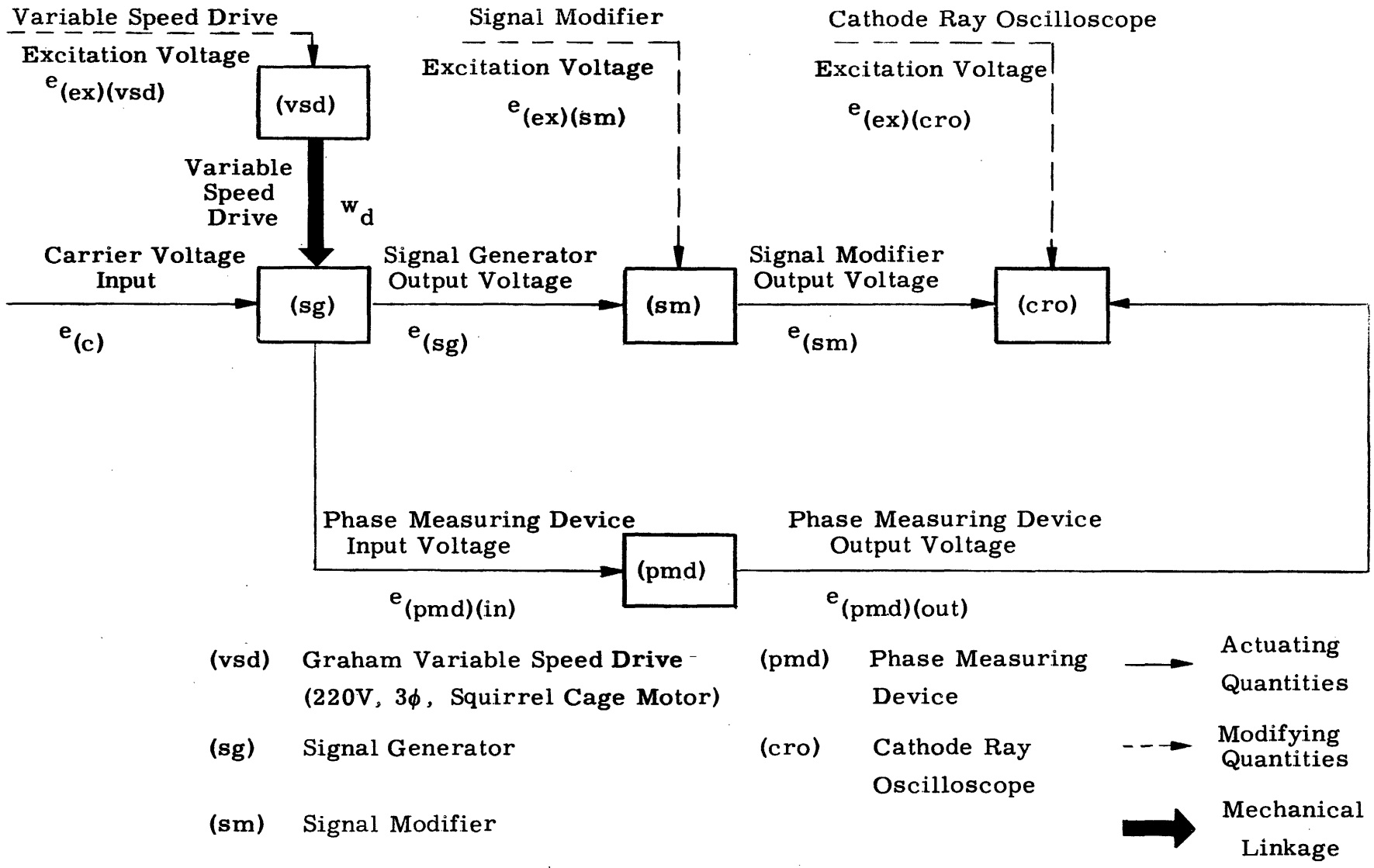

Fig. A-7 Functional Diagram for Experimental Set Up Using A.C. Chopper Network as a Signal Modifier.

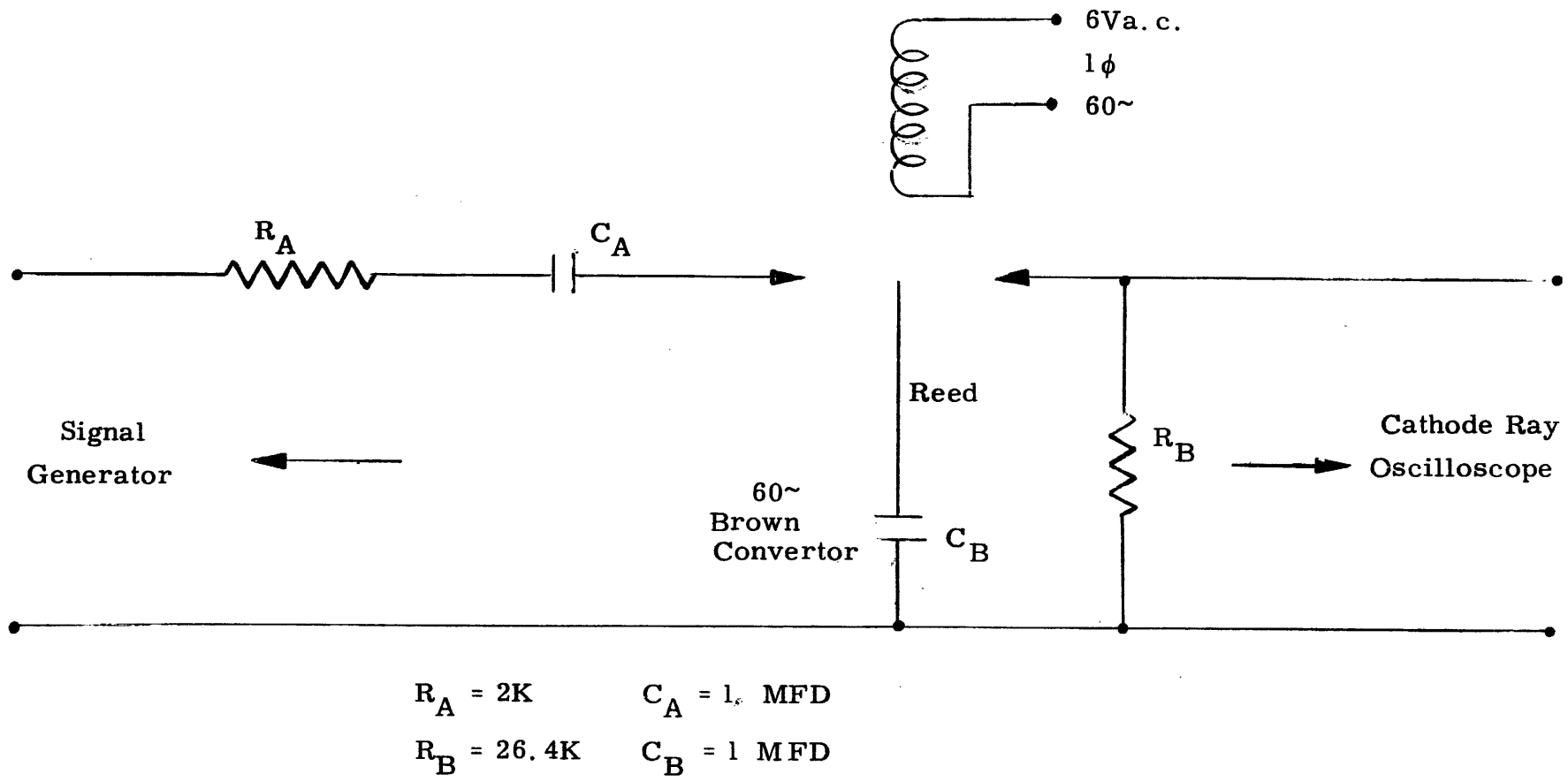

Fig. A-8 Schematic Diagram of the Chopper R C Signal Modifier of Type II.

APPENDIX B

EXPERIMENTAL FREQUENCY RESPONSE CHARACTERISTICS FOR THE SIGNAL MODIFIERS ANALYZED

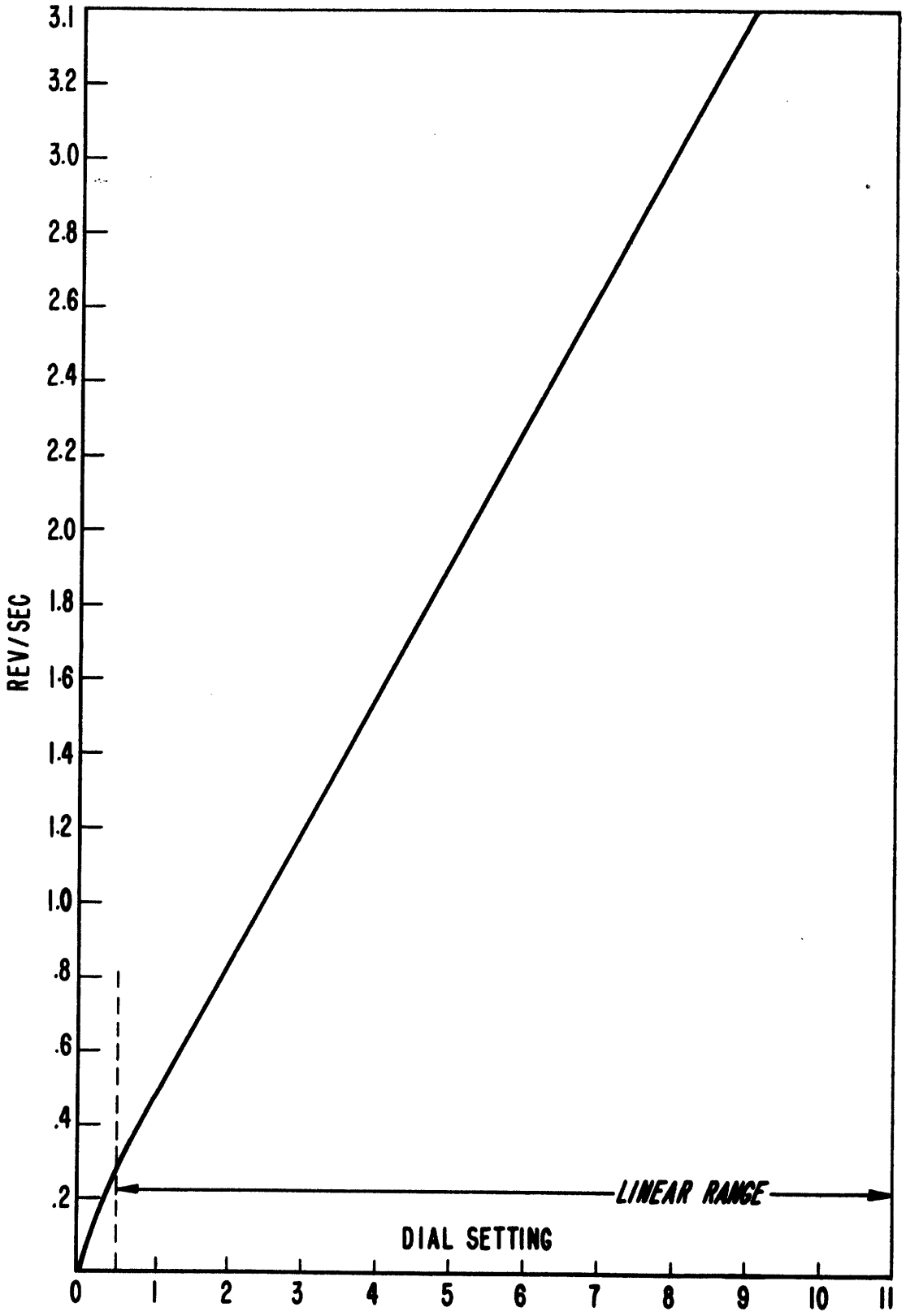

Fig. B-1 Dial calibration for the Graham Variable Speed Drive

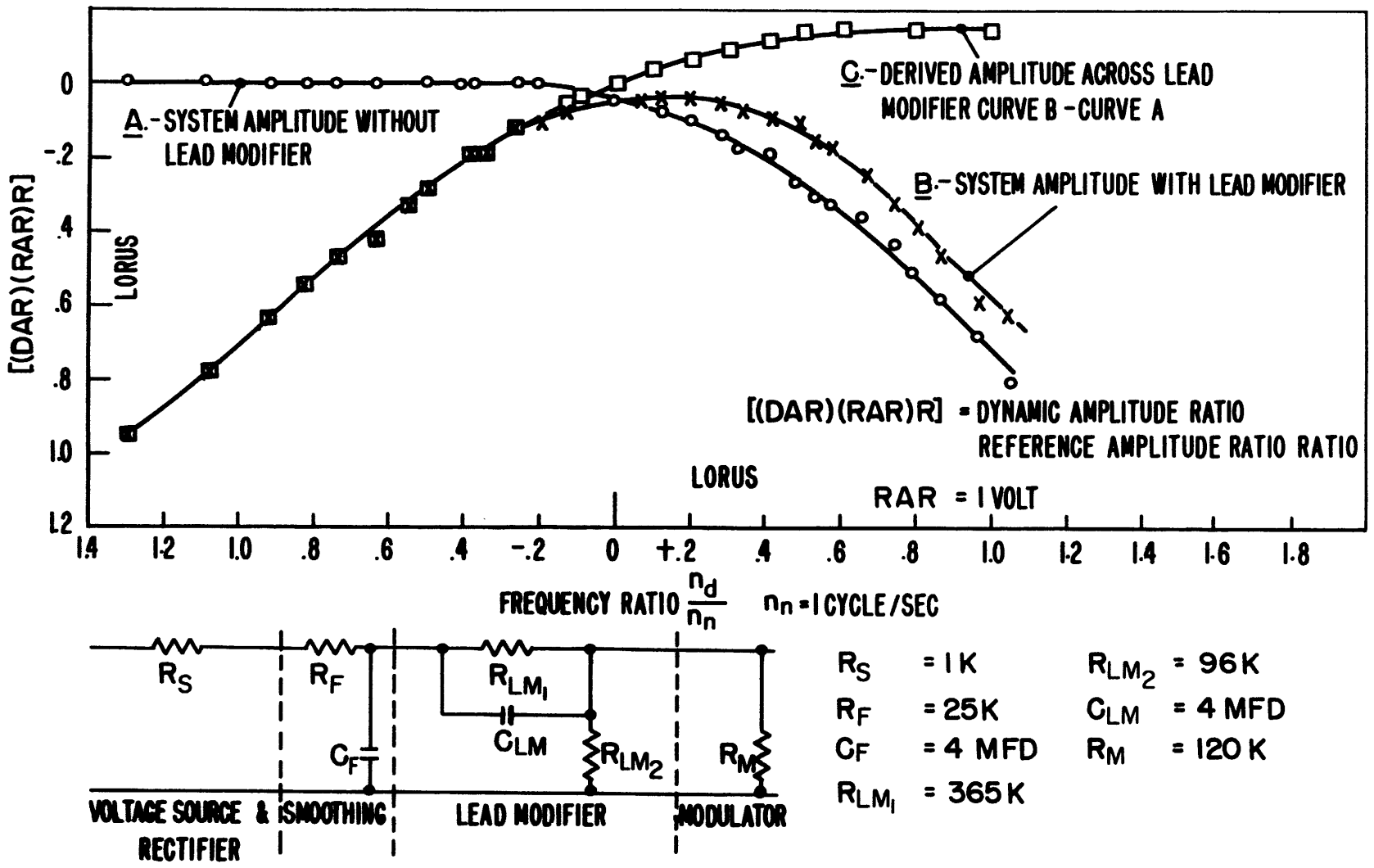

Fig. B-2 Amplitude response for Type I System

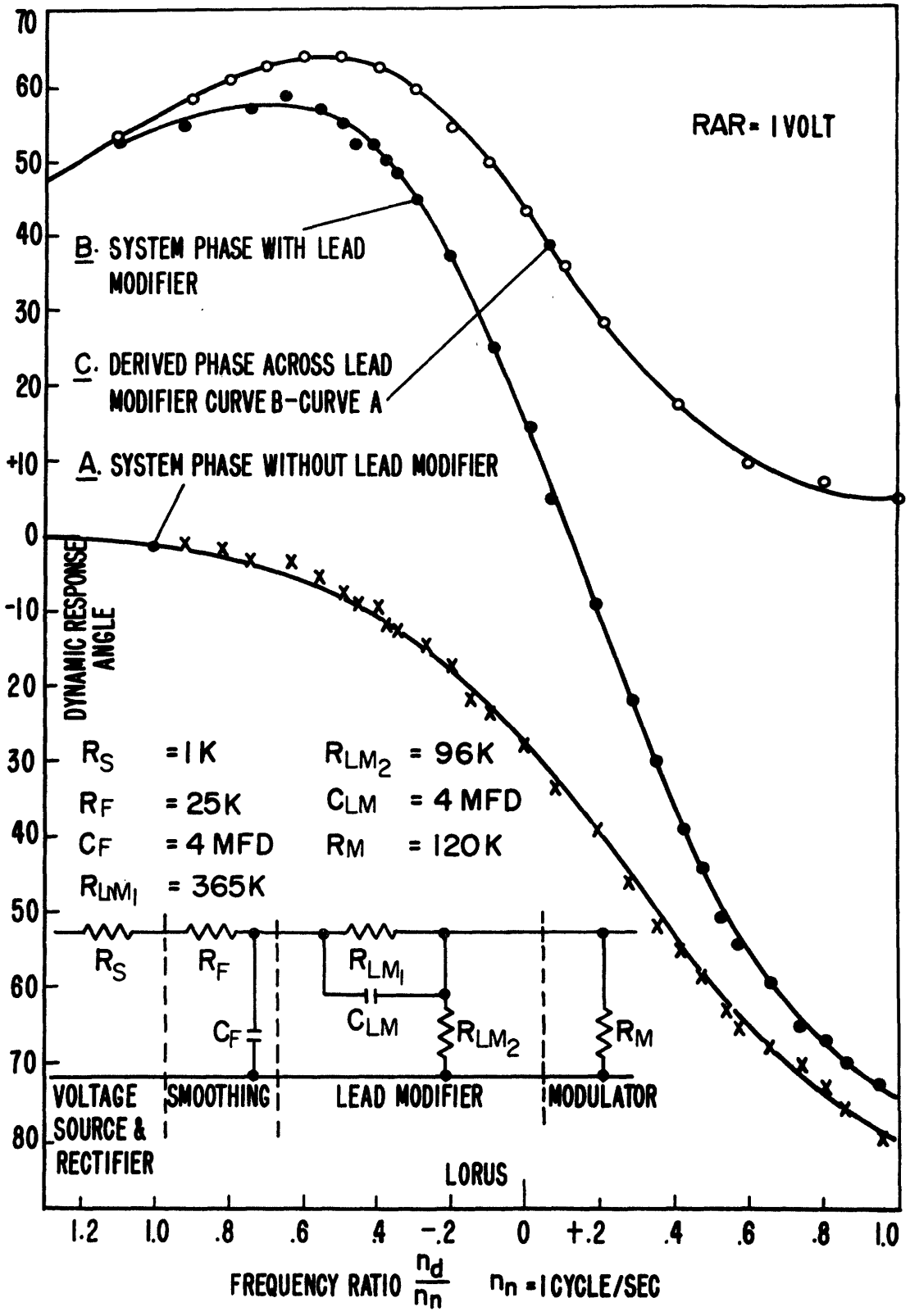

Fig. B-3 Phase response for Type I system

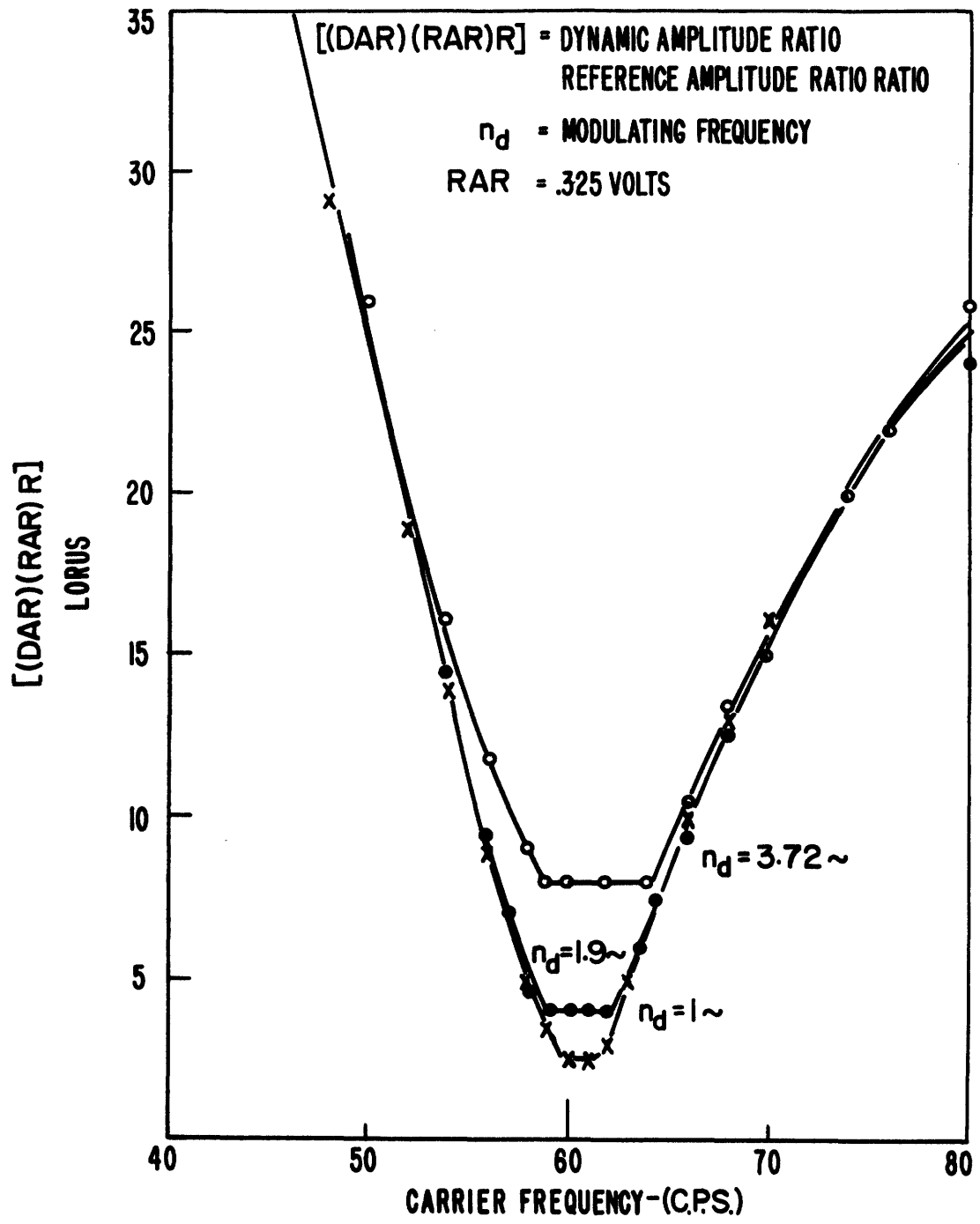

Fig B-4 Amplitude-carrier frequency response characteristics of the parallel "T" signal modifier for different modulating frequencies. Parallel "T" tuned to 60 cycles.

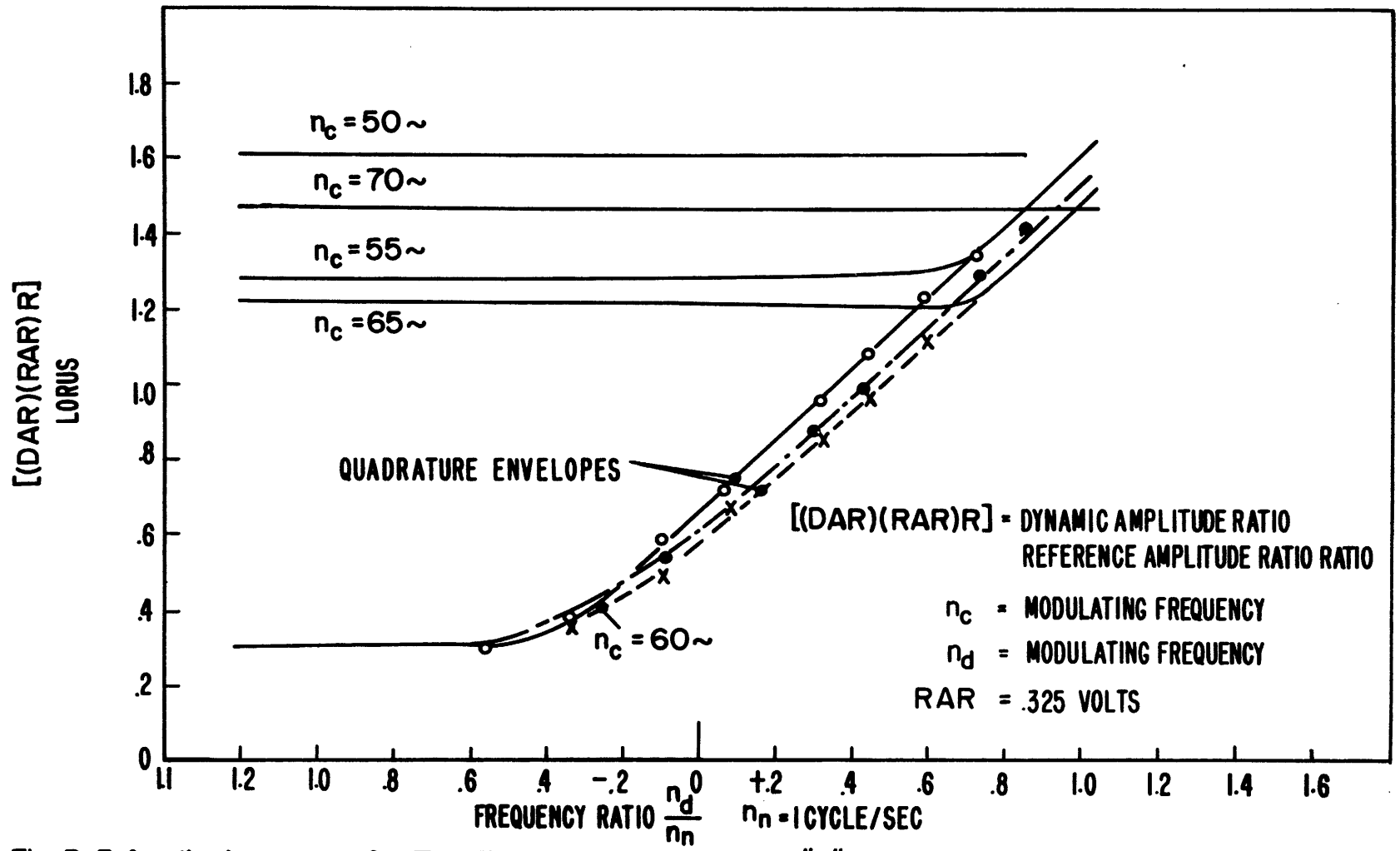

Fig. B-5 Amplitude response for Type II system using a parallel "T" signal modifier, for various carrier frequencies. Parallel "T" tuned to 60 cycles.

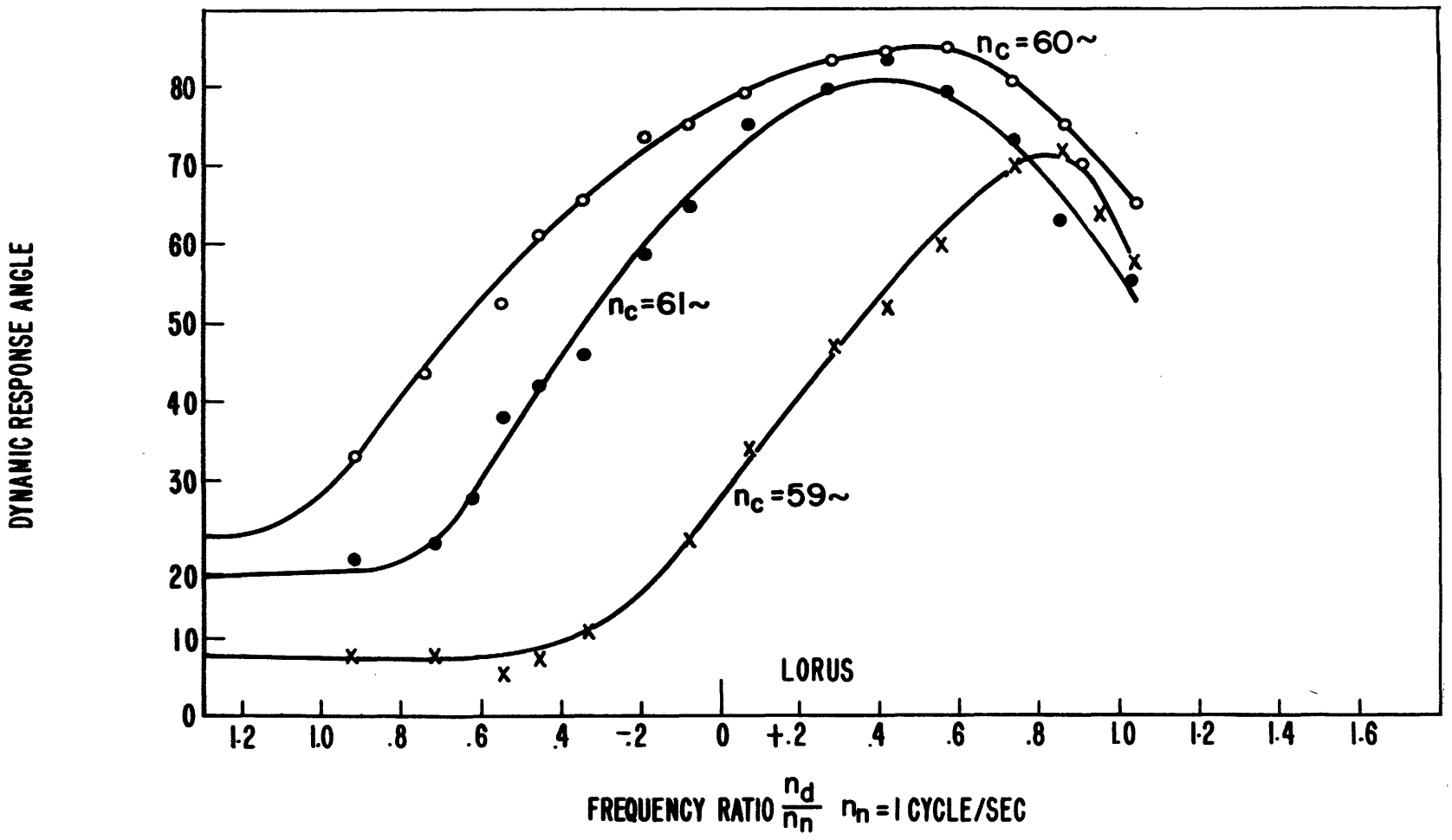

Fig. B-6 Phase response for Type II system using a parallel "T" signal modifier for various carrier frequencies. Parallel "T" tuned for 60 cycles.

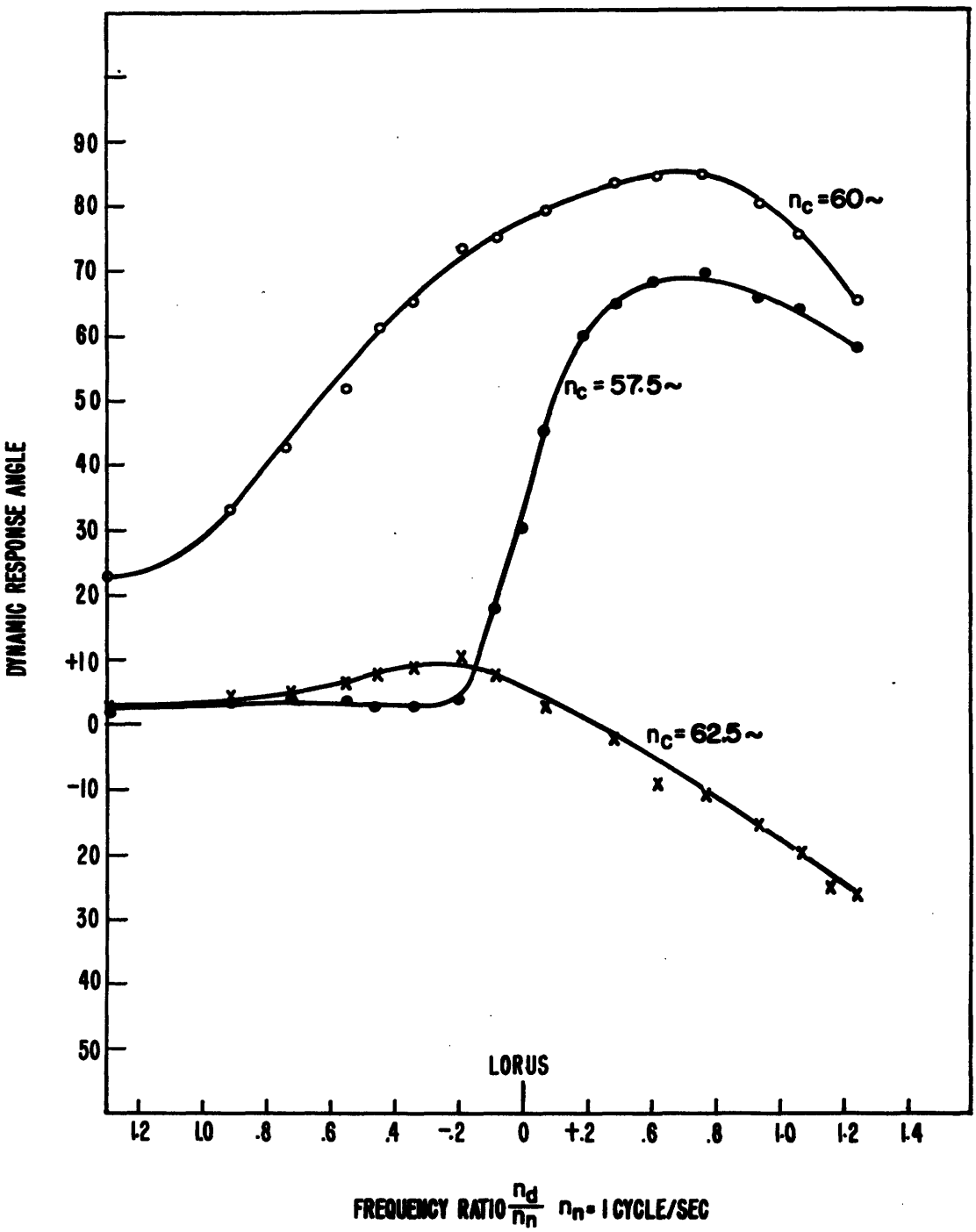

Fig. B-7 Phase response for Type II system using a parallel "T" signal modifier for various carrier frequencies. Parallel "T" tuned for 60 cycles.

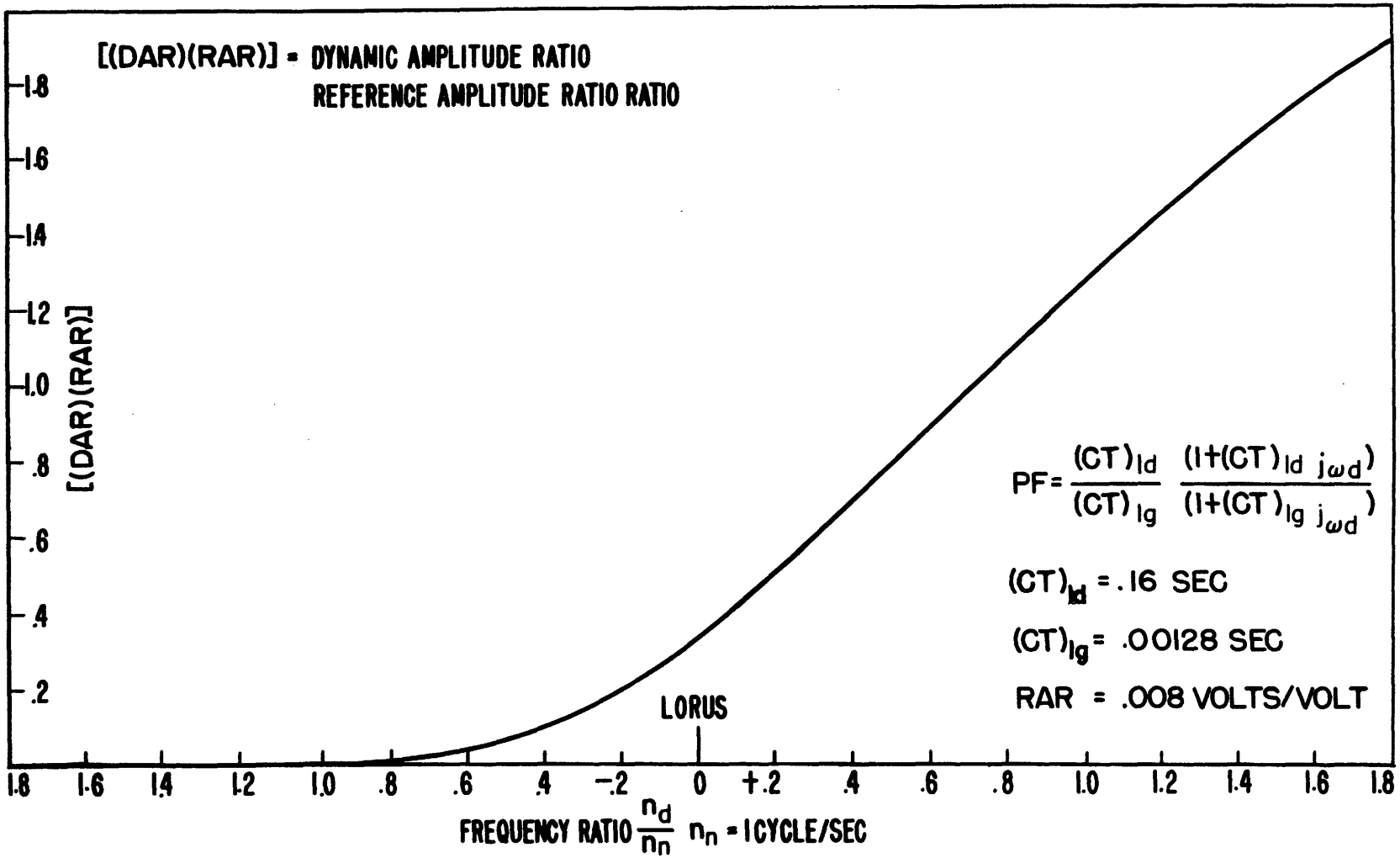

Fig B-8 Theoretical first order amplitude response for the parallel "T" signal modifier tuned to 59.5 cycles

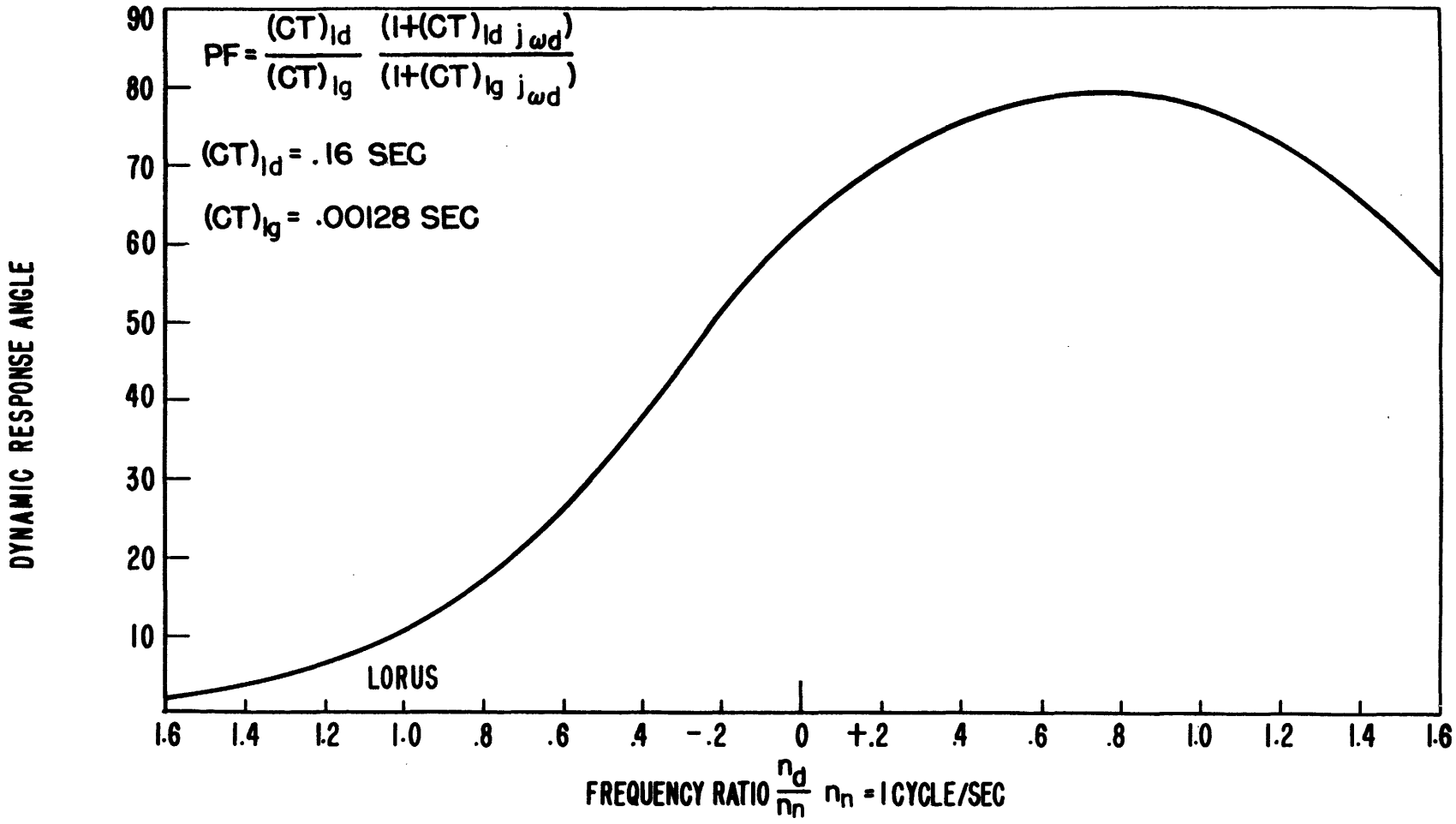

Fig. B-9 Theoretical first order phase response for the parallel "T" signal modifier tuned to 59.5 cycles.

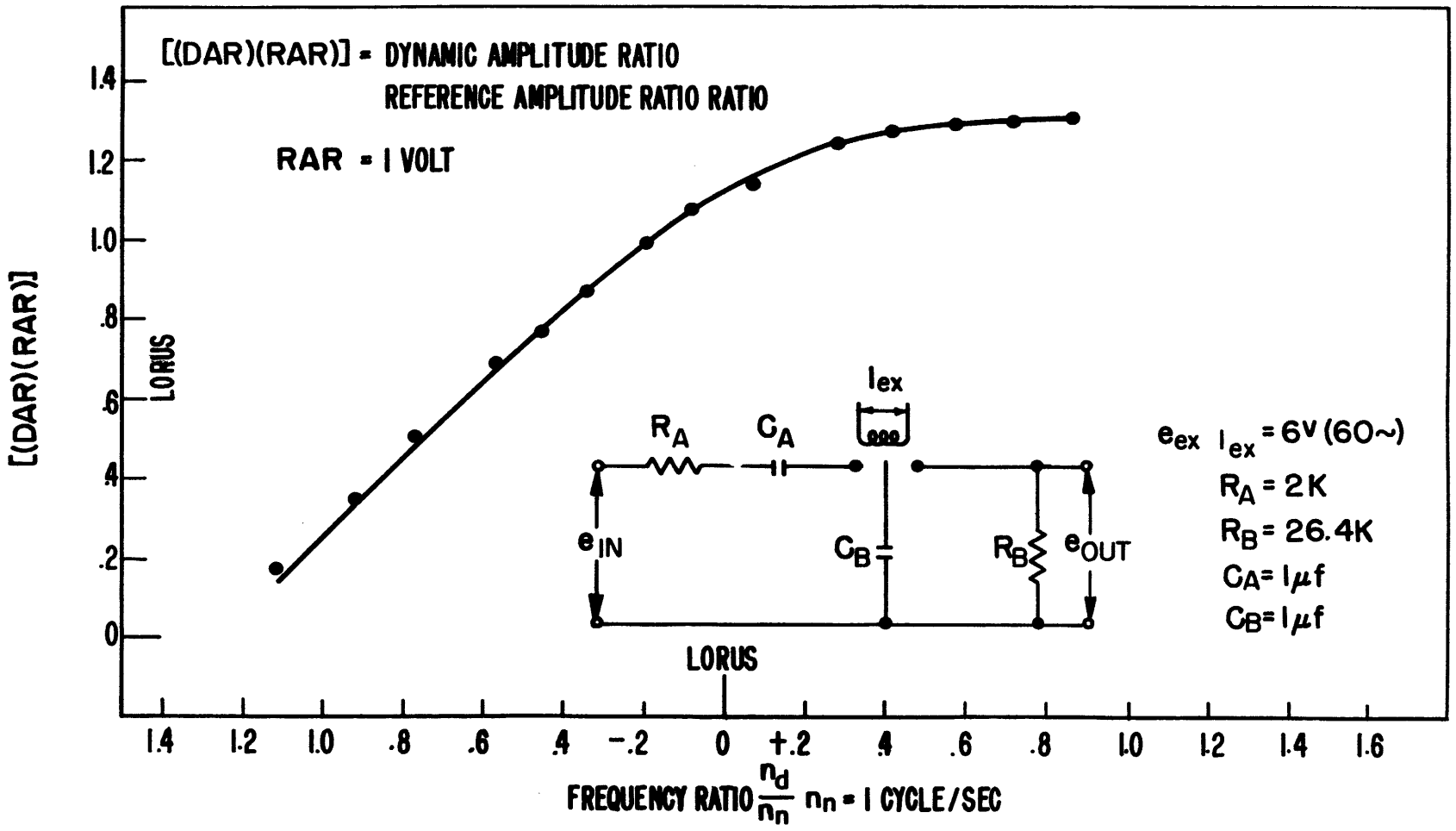

Fig. B-10 Amplitude response for Type II System using a chopper rate circuit

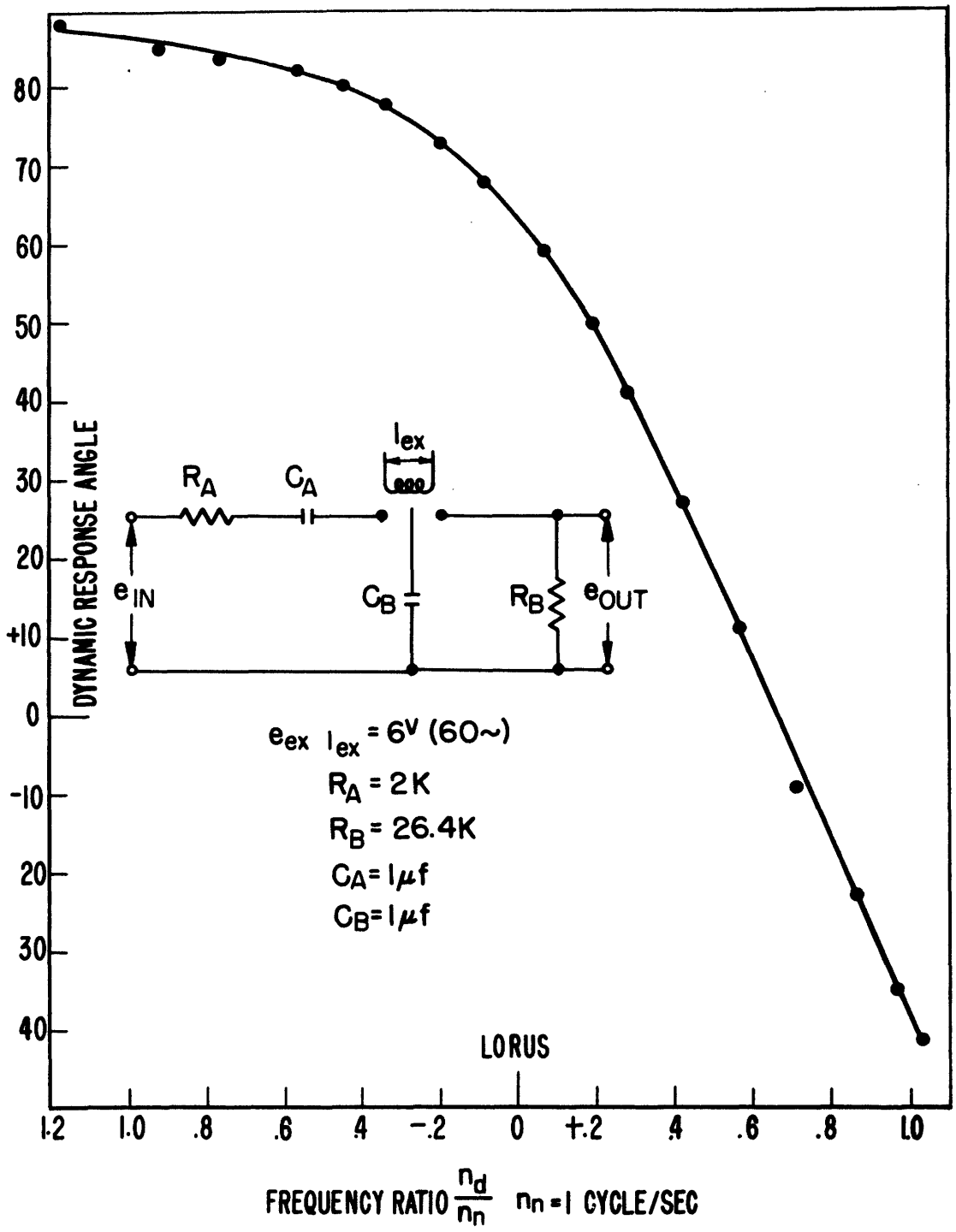

Fig. B-11 Phase response for Type II System using a chopper rate circuit

APPENDIX C

RECOMMENDATION

Since, in the type I system, phase lag, introduced by the smoothing filter, was the limiting factor in obtaining lead at higher frequencies, and noise, primarily due to quadrature voltages introduces by rectification, is a limiting factor in the useful signal available at lower frequencies, the followin is offered for future consideration.

A suppressed carrier modulated wave has the form f(t) cos $w_c t$. The desired information is f(t) and can be obtained if f(t) cos $w_c t$ be multiplied by sec $w_c t$. To do this electrically would require infinite gain at $w_c t = 90^o$. This of course is not practical. Even if a very high gain is obtained, sec $w_c t$ would be multiplying f(t) cos $w_c t$ when the amplitude of the modulated wave is almost equal to its noise level. Consequently, the noise would be multiplied too.

However, conisder the following:

(1) let f(t) = cos $w_d t$.

(2) Multiply cos $w_d t$ cos $w_c t$.by $\frac{5 \ -3\cos w_c t}{2}$

$\frac{5 \ -3\cos w_c t}{2}$ is a very close approximation to sec $w_c t$ for $-45^o < w_c t < 45^o$. Then full wave rectify, and chop out 90^o segments from the rectified waves. Filter the output of the chopper. Fig. C-1, 2, 3, 4 illustrate this, except that the rectification is shown performed first for illustrative purposes.

Cos $w_d t$ cos $w_c t$ fully rectified

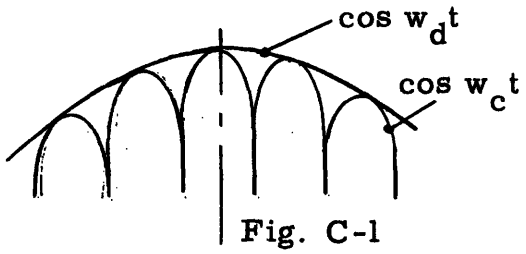

Fig. C-1

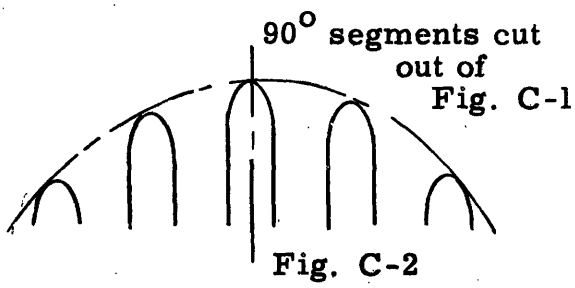

Fig. C-2

Comparison of fig. C-4 to fig. C-5 shows that there is less ripply and less lag with the recommended method of preparing a signal for Type I signal modification. It may be worthy of investigation.

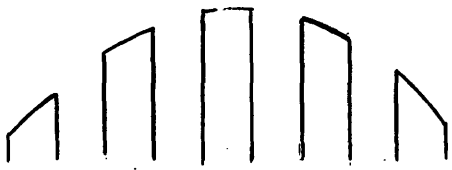

Fig. C-3

Multiplying Fig. C-2 by $\left|\frac{5-3\cos w_c t}{2}\right|$

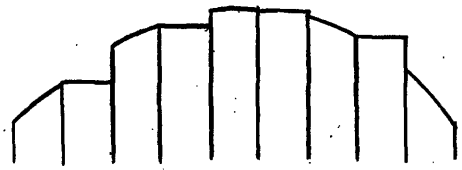

Fig. C-4

The filtered output. The input wave form to the filter is that of Fig. C-3.

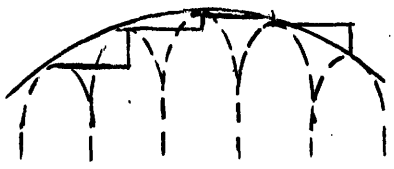

Fig. C-5

The filtered output of a normally rectified wave.

APPENDIX D

OPERATION OF THE DIODE BRIDGE

The bridge is constructed as indicated in Fig. D-1. Consider first that no signal is applied. If the potentiometers are balanced, equal currents flow through each of the pairs of tubes during their conducting periods. That is, the tubes are available for conducting in pairs, one pair presents a low impedance path each half cycle. The effect of different tube characteristics is minimized by the large loading impedances and by the parallel current paths.

When a signal is applied to terminals A and B, the polarity of the applied signal with respect to the plate voltage determines the direction of the output voltage. A low frequency signal and a higher frequency plate voltage will produce a suppressed carrier modulated output except that the carrier component will have the characteristics shown in Fig. D-2.

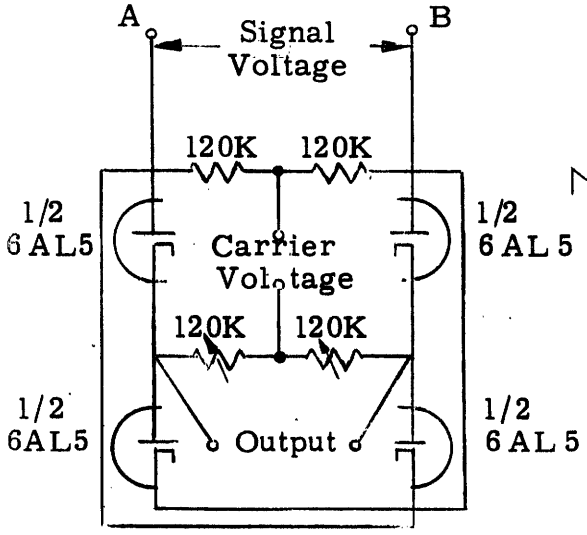

Fig. D-1 Diode Bridge

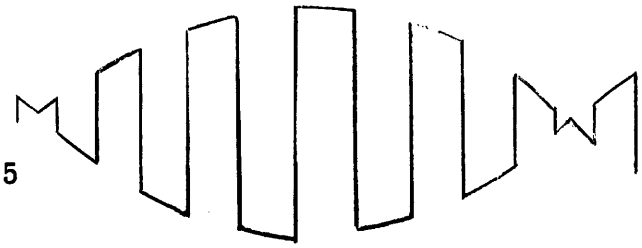

Fig. D-2 Output Wave Form

BIBLIOGRAPHY

1. H.M. James, N.B. Nichols, and R.S. Phillips, Theory of Servomechanisms, Chapter 3, McGraw-Hill Book Company, Inc., N.Y., N.Y., 1947

2. G.M. Attura, Effects of Carrier Shifts on Derivative Networks for A-C Servomechanisms, Transactions of the American Institute of Electrical Engineers, Volume 70, Part I, Page 612, 1951.

3. A. Sobezyk, Stabilization of Carrier Frequency Servomechanisms, Franklin Institute Journal, Volume 246, Pages 21, 95, and 187, 1948.

4. W.R. Ahrendt, Servomechanism Practice, Chapters 3, 6, and 17, McGraw-Hill Book Company, Inc., N.Y., N.Y., 1954.

5. H. Lauer, R. Lesnick, and L.E. Matson, Servomechanism Fundamentals, Chapter VI, McGraw-Hill Book Company, Inc., N.Y., N.Y., 1947.

6. A.P. Notthoff, Jr., Phase Lead for A-C Servo Systems with Compensation for Carrier Frequency Changes, Transactions of the American Institute of Electrical Engineers, Volume 69, Part 1, Page 285, 1950.

7. D. McDonald, Improvements in the Characteristics of A-C Lead Networks for Servomechanisms, Transactions of the American Institute of Electrical Engineers, Volume 69, Part 1, p. 293, 1950.

8. A.C. Donovan, Alternating Current Rate Circuit, Engineering Notes E-110, Instrumentation Laboratory, Massachusetts Institute of Technology, Cambridge, Massachusetts, September 1951.

9 S.S. Seely, Electron-Tube Circuits, Chapter 14, McGraw-Hill Book Company, Inc., N.Y., N.Y., 1950.

10. W.L. Pragnell, Measurement of Dynamic Angle in Servo Systems, Engineering Notes E-190, Instrumentation Laboratory, Massachusetts Institute of Technology, Cambridge, Massachusetts,

11. M.H. Goldstein, Sensitivity-function Analysis of Modulation System with Statistical Inputs, M.I.T. Master's Thesis, Electrical Engineering Dept., 1951.

12. L. Christiansen, Cubic Distortions in Ring Modulators, Electrical Communications, International Telephone and Telegraph Corporation, N.Y., N.Y., March, 1955.

13. C.S. Draper, W. McKay, S. Lees, Instrument Engineering, Volume II, Chapter 19, McGraw-Hill Book Company, Inc. N.Y., N.Y., 1953.